National Aeronautics and
Space Administration

NASA CR-174990
R86AEB104

IMPROVED FRACTURE TOUGHNESS CORROSION-RESISTANT BEARING MATERIAL

FINAL REPORT

By
E.N. Bamberger
A.H. Nahm

JANUARY 1986

GENERAL ELECTRIC COMPANY
AIRCRAFT ENGINE BUSINESS GROUP

Prepared For
NATIONAL AERONAUTICS AND SPACE ADMINISTRATION
LEWIS RESEARCH CENTER
21000 BROOKPARK ROAD
CLEVELAND, OHIO 44135

Contract
NAS3-22508

(NASA-CR-174990) IMPROVED FRACTURE TOUGHNESS CORROSION-RESISTANT BEARING MATERIAL Final Report, 1981-1984 (General Electric Co.) 81 p CSCL 13I

N86-32743

Unclas
G3/37 44625

FOREWORD

This program was performed under NASA Contract 3-22508. The NASA project managers were Mr. R.J. Parker and Mr. H. Coe.

The authors acknowledge the significant contributions of Mr. R. Hodder, D. Maloney, and Dr. R. Klundt of Latrobe Steel Co., Latrobe, PA, and Drs. T.B. Cameron and D. Diesburg of AMAX Research Center, Ann Arbor, Michigan. Lastly, the author thanks Mr. D. Kroeger of General Electric EMTL for his contributions to the overall effort.

TABLE OF CONTENTS

PRECEDING PAGE BLANK NOT FILMED

LIST OF ILLUSTRATIONS

LIST OF ILLUSTRATIONS (Continued)

LIST OF ILLUSTRATIONS (Continued)

LIST OF ILLUSTRATIONS (Concluded)

LIST OF TABLES

1.0 SUMMARY

This report documents a development effort designed to achieve a corrosion resistant improved fracture toughness bearing alloy. At the outset of the program the decision was made to modify a 14Cr steel (AMS 5749) by reducing its carbon level to a point where carburizing became feasible. By creating a bihardness material, it was felt that the requisite conditions for a fracture-tough bearing material could be achieved. In addition, the use of a high chromium content material to achieve this would provide the desired corrosion resistance. Lastly, it was anticipated that the beneficial residual compressive stresses created by carburizing and subsequent heat-treatment would act to improve rolling contact fatigue, as would the reduction in the size and quantity of insoluble carbides normally found in the high-carbon AMS 5749.

Development efforts were not successful in achieving the above goals. It was recognized at the outset that the high Cr content posed a severe problem to carburization. While this was and is a major problem, some of the carburizing cycles did result in acceptable microstructures or case hardnesses. The operational word here is "or," since the necessary combination of good microstructure (such as relatively small, well dispersed carbides, with no network or agglomeration) and adequate hardness ($> R_c$ 58 minimum) was not attained.

Initially, only the carbon level was reduced, resulting in a low carbon AMS 5749. It was quickly evident that this chemistry was totally unsuitable for carburizing, the main problem being one of uncontrollable and massive amounts of retained austenite.

A successful portion of this initial effort was the development and demonstration of a modified corrosion test (based on a USN procedure) which provided useful data on the relative corrosion characteristics of AMS 5749, AISI M50, and 52100 bearing steels.

The second alloy modification consisted of adding approximately 3% by weight nickel, the intent being to help reduce the retained austenite levels. This modification resulted in considerably improved structures and hardness levels and generally more repetitive results. Still, the ideal combination of microstructure and hardness was not achieved.

A final attempt at achieving a fracture-tough, inherently corrosion-resistant material was made by evaluating a number of lower chromium (8% to 12% weight), low carbon alloys. Again, the results were mixed. While it was shown that the lower Cr alloys had good inherent corrosion characteristics (compared to M50), the desired microstructure and hardness combination was still not attained.

2.0 INTRODUCTION

This program was launched with the intent of providing a corrosion resistant, high fracture toughness bearing material for advanced jet engine and other critical applications.

Corrosion of aerospace bearings is a serious and expensive problem: it is most severe in systems with long periods of nonuse. A summary of causes for bearing rejection at a U.S. Navy facility shows that corrosion accounts for nearly one-third of the bearing rejections from their aircraft systems, including drive lines, wheels, and accessories (Reference 1). Air Force experience confirms that corrosion is a major cause of rejection at overhaul of aircraft turbine engine bearings (Reference 2).

Cryogenic turbopump bearings in current and future rocket engines, such as the space shuttle main engine, also require the use of corrosion resistant bearings. AISI 440C is currently used for bearings in cryogenic applications. Its hardness, fatigue life, and load capacity make AISI 440C a marginal material for future cryogenic turbopump bearings and also inadequate for turbine-engine main-shaft bearings. A significant mechanism of corrosion in aircraft engine bearings was defined (References 3 and 4) as a result of observations from Naval fleet aircraft bearings. It was concluded that the corrosion responsible for bearing rejections was caused by cyclic temperatures and lengthy static periods frequently experienced by aircraft in the field. The temperature of the lubricant in these engines can cycle from 508 K (455° F) during operation to 233 K (-40° F) during inactive periods in cold climates. Moisture-laden air can get into the lubrication system in humid environments, during rain, or during aircraft water wash; moisture can condense on bearing components during inactive periods. Additionally, it was found (References 3 and 4) that up to 3 ppm of chloride ion (most likely from sea water) was contained in the lubricant. Observations of rejected bearings showed that the corrosion was concentrated at the crevice formed by the contacts of the balls or rollers and the raceways. The lubricant and condensate containing the chloride ion settled in this area and crevice corrosion occurred. The presence of chloride ions accelerates corrosion (Reference 5).

Although these observations were limited to bearings in Naval aircraft, it is likely that a similar mechanism occurs in other aircraft and aerospace bearings rejected for corrosion. If the corrosion pits are of significant size, they can act as initiation sites for fatigue spalling, thereby shortening bearing life.

The corrosion problem is being attacked on three major fronts: corrosion-resistant materials, corrosion-resistant coatings or surface modifications, and corrosion-inhibited lubricants. Materials such as AISI 440C, AMS 5900, and AMS 5749 are called corrosion-resistant or stainless steels; however, under some severe environmental conditions in aircraft bearings, corrosion will occur. Nevertheless, they are significantly more corrosion-resistant than common aircraft bearing materials like AISI M50, AISI 52100, and the commonly used case-carburized materials. Ceramics like silicon nitride are truly corrosion-resistant in an aircraft environment. Although this material is not yet well developed for widespread aircraft application, it could be applied in some specific cases.

Chromium-ion implantation has shown significant improvement in the corrosion resistance of AISI M50 (Reference 6). Other surface modifications or coatings may also provide similar benefits, but more work is needed in this area. It is probable that a combination of approaches, such as the use of silicon nitride balls or rollers and coated raceways, may be a workable solution for some applications requiring long periods of nonuse.

Currently, the lubricant provides some measure of corrosion protection in aircraft bearings simply by keeping the components coated and moisture free. Corrosion-inhibiting additives for the commonly used MIL-L-23699 lubricant have shown promise in laboratory tests (References 3 and 4), and confirmation of the degree of improved corrosion resistance in actual aircraft systems is underway.

Such steels as AMS 5749 and AMS 5900 combine the tempering, hot hardness, and hardness-retention characteristics of AISI M50 steel with the corrosion and oxidation resistance of AISI 440C stainless steel. The typical chemical compositions of these materials are shown in Table 1. For improved corrosion and wear resistance, AMS 5749 and AMS 5900 steels contain higher percentages of carbon and chromium than AISI M50. Their hot hardness and hardness retention are better than AISI 440C and similar to AISI M50 (Reference 7).

Table 1. Chemical Compositions of Test Materials.

	C	Mn	Si	Cr	Mo	V	Ni	S	P
CEVM AISI 52100	1.04	0.34	0.30	1.46	0.03	----	0.04	0.003	0.008
VIM-VAR AISI M50	0.82	0.28	0.24	4.20	4.16	1.01	0.08	0.002	0.007
VIM-VAR AMS 5749	1.11	0.17	0.30	13.92	3.87	1.15	0.01	0.003	0.003

AMS 5749 and AMS 5900 showed excellent life in several accelerated rolling-element fatigue studies (References 7 to 10). These materials were double vacuum-melted (VIM-VAR for vacuum induction melt-vacuum arc remelt) and showed lives equal to or greater than VIM-VAR AISI M50 in similar tests. These life results are significant because they show that a corrosion-resistant material that could potentially replace AISI M50 in some aircraft bearing applications would be expected to have at least equivalent lives.

The need for high fracture toughness bearings has been discussed in detail in References 11 and 12. Materials like General Electric's M50NiL have adequately solved this problem, but without improving corrosion resistance. M50NiL is derived from AISI M50 and, having the same chromium and molybdenum content, has the same corrosion characteristics. To achieve an inherently corrosion-resistant material, a high chromium content steel, such as the 14Cr AMS 5749, needs to be considered. The major objective of this program was to link the corrosion resistance of a 14Cr steel with the high fracture resistance possible with a case-carburized material. A second objective was to evaluate the corrosion resistance of AMS 5749 relative to AISI M50 and AISI 52100.

The first efforts were focused on a reduced carbon level AMS 5749 material. A second alloy modification consisted of adding a small amount of nickel; a third development attempt involved the evaluation of several lower chrome (<14%), low carbon alloys. Most of these materials were subjected to the corrosion test procedures developed as part of this program. The results of these investigations and evaluations are discussed in the following sections of this report.

3.0 MATERIAL DEVELOPMENT RESULTS AND DISCUSSION

The corrosion test procedures and results will be discussed first, followed by the material development and modification program.

3.1 CORROSION TESTING

The extent of corrosion resistance improvement of the 14Cr materials over the more common aircraft bearing materials like AISI M50 and AISI 52100 has not been well documented or published. Consequently, at the outset of the current program it was decided to establish a corrosion test procedure to obtain baseline data relative to the corrosion characteristics of AMS 5749 and such materials as AISI M50 and 52100. In addition, corrosion tests were performed on the low carbon and nickel modified versions of the AMS 5749, as well as some of the experimental alloys evaluated in the latter stages of this program.

The corrosion test selected was similar to the one described in Reference 3. This procedure, as developed by the Navy, has been proven to provide a realistic assessment of the relative corrosion characteristics of bearing and gear materials. It should be noted that the initial baseline corrosion tests (those with through-hardened AMS 5749, M50, and 52100) have been reported in Reference 13.

The evaluation was performed by conducting a series of corrosion tests with specimens fabricated to simulate crevice corrosion in the presence of a specially prepared lubricant-chloride solution and exposed to thermal cycling.

3.1.1 Test Materials

The chemical composition of the materials used in these tests was given in Table 1. Thirteen mm (0.5 in) diameter bar stock was heat treated to obtain a nominal Rockwell C hardness of 62. The specific heat treat cycles are described in Table 2. Cylindrical bars 76.2 mm (3.0 in) long and 9.5 mm (0.375 in) in diameter were then ground from the heat treated rods. Half of the test bars were machined with saddles as shown in Figure 1 with a radius slightly greater than the bar radius. This saddle provides a contact and crevice situation to simulate the contact of a ball or roller and a bearing raceway. Both the cylindrical and the saddle surfaces were ground to a finish of 0.15 μm (6 μin).

The lubricant used for the corrosion tests consisted of MIL-L-23699 type lubricant to which was added 3 ppm by weight of chlorides (supplied as ASTM D665 synthetic seawater). The water content of the lubricant solution was then adjusted to 600 ppm by weight by the addition of distilled water.

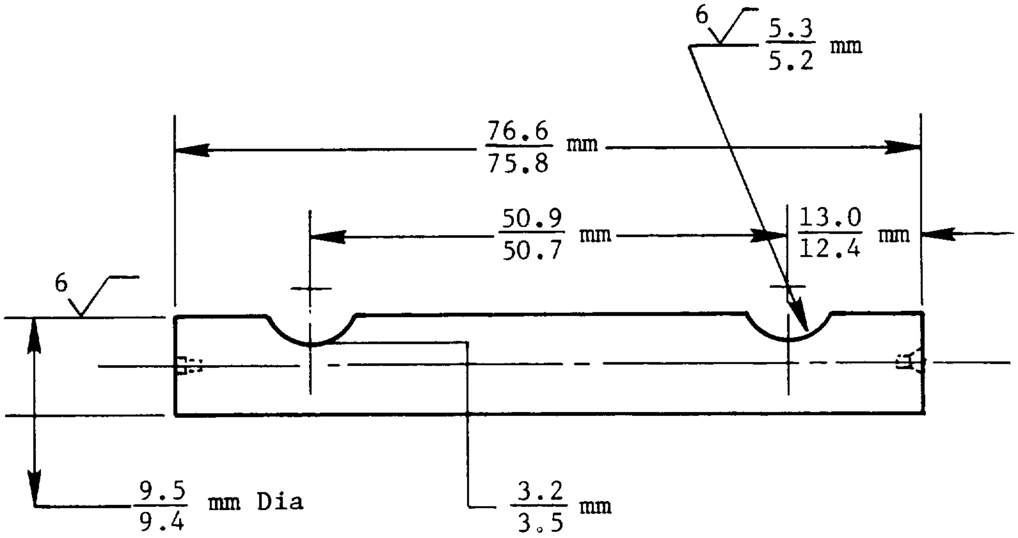

Grooves to be Parallel Within 0.05 mm

Figure 1. Corrosion Test Specimen.

Table 2. Heat Treatment of Test Materials.

Heat Treatment	Material		
	AISI 52100	AISI M50	AMS 5749
Preheat	None	1089 K (1500° F) in Salt	1089 K (1500° F) in Salt
Austenitize	1116 K (1550° F) in Salt	1380 K (2025° F) in Salt	1394 K (2050° F) in Salt
Quench	327 K (130° F) Oil, Air Cool to Room Temperature	839 K (1050° F) in Salt, Air Cool to Room Temperature	866 K (1100° F) in Salt, Air Cool to Room Temperature
Temper	450 K (350° F) for 2 Hours	797 K (975° F) for 2 Hours	811 K (1000° F) for 2 Hours
Deep Freeze	200 K (-100° F) for 2 Hours	200 K (-100° F) for 2 Hours	200 K (-100° F) for 2 Hours
Temper	450 K (350° F) for 2 Hours	797 K (975° F) for 2 Hours	811 K (1000° F) for 2 Hours

3.1.2 Corrosion Test Procedure

The procedure used for these corrosion tests was similar to that used in Reference 3. The test bars of each material were cleaned by successively washing in separate baths of toluene, ethanol, hexane, and acetone. Afterward, the bars were handled only by rubber-gloved hands and were air-dried at room temperature. Next, the bars were immersed for 1 hour in the lubricant-chloride solution. During exposure, they were periodically rotated. The bars were removed and drained for 30 minutes at room temperature.

Subsequently, the bars were placed in a special fixture, shown schematically in Figure 2 and photographically in Figure 3, with the lower two bars having the saddle and the mating two bars placed across the saddles. This arrangement produces a contact and crevice situation similar to that in a ball or roller bearing, and it provides the opportunity for crevice corrosion to occur. The fixture is made of polyethylene material; it is clamped together and suspended in a large beaker which is loosely covered with aluminum foil. This assembly is called the corrosion cell and is cycled alternately between a 339 K (150° F) oven and a 276 K (37° F) refrigerator. Total exposure is 14 cycles, each cycle consisting of 8 hours in the oven and 16 hours in the refrigerator. Corrosion cells were assembled with each of the three materials.

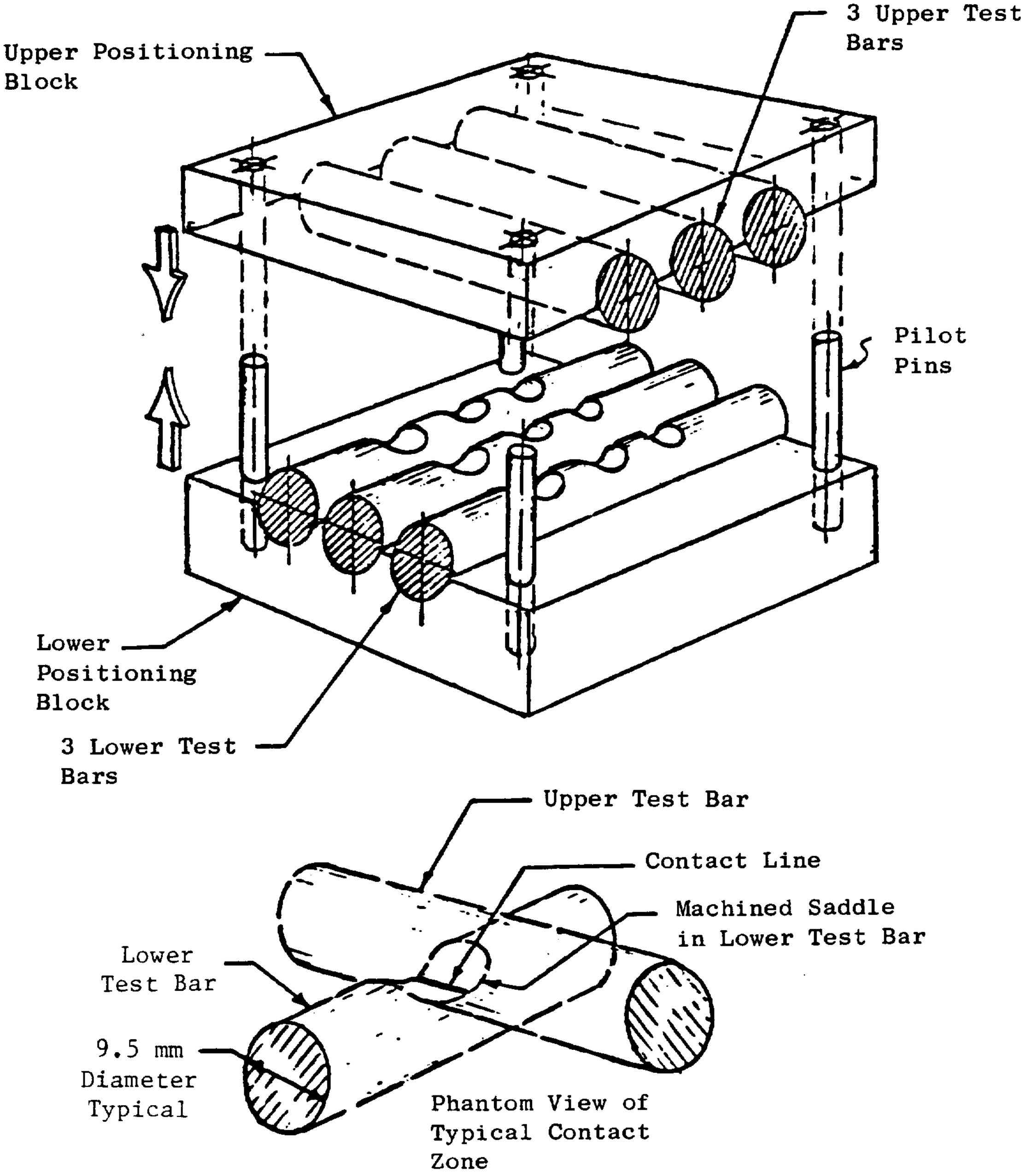

Figure 2. Corrosion Test Fixture.

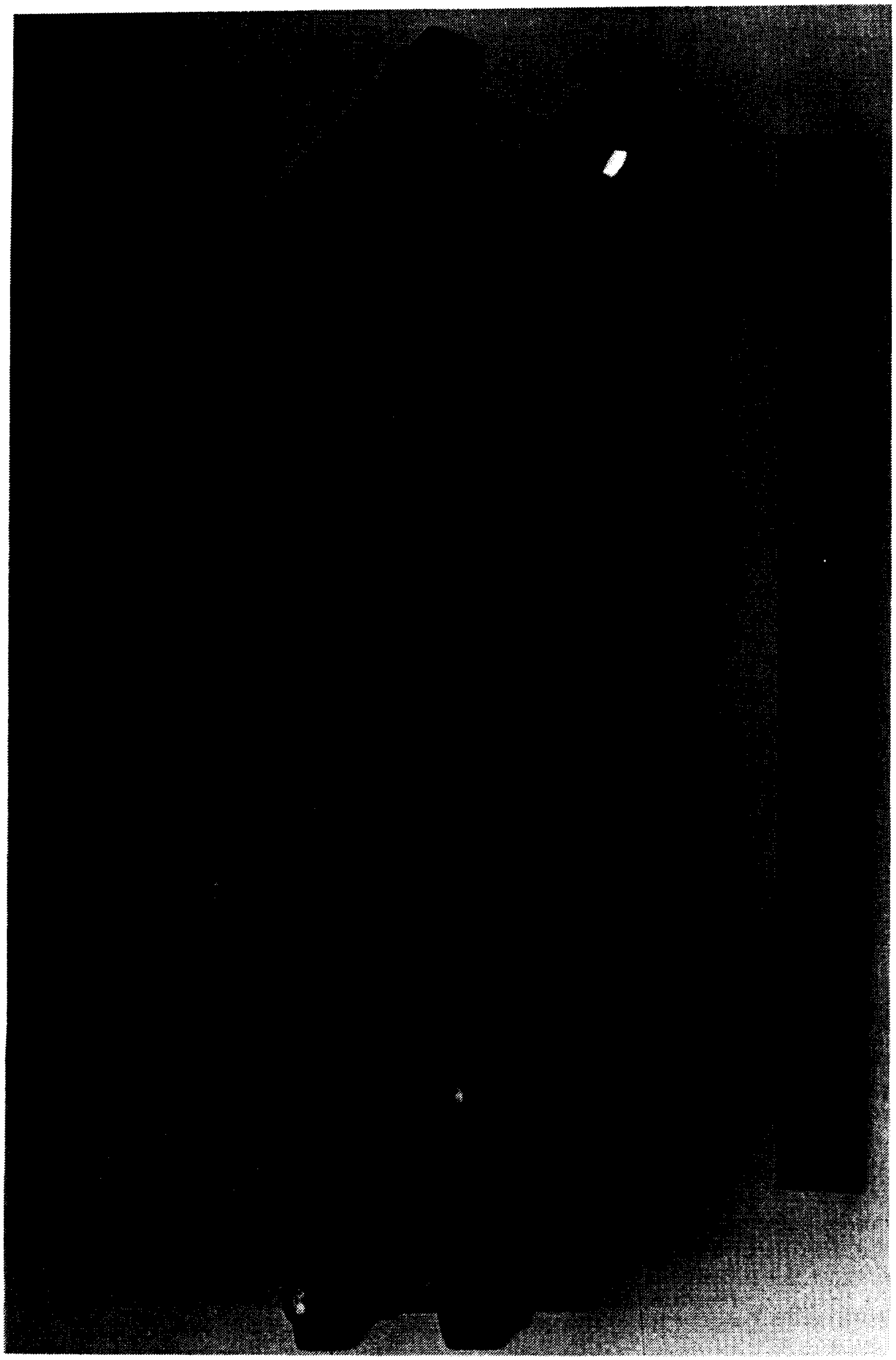

Figure 3. Corrosion Test Assembly With Test Bars.

After completing the exposure, the bars were removed, cleaned with an alkaline solution in an ultrasonic cleaner, and photographed. Typical corrosion sites were examined metallographically to determine corrosion characteristics.

3.1.3 Corrosion Test Results

After the 14 thermal cycles were completed, the test bars were cleaned and examined. Visual inspection revealed that the AISI M50 and AISI 52100 had extensive corrosion damage. A slight amount of corrosion was present on the AMS 5749 bars. As shown in Figures 4 through 6, corrosion was not limited to crevice corrosion, but pitting corrosion also occurred on exposed surfaces of both materials. The slight amount of corrosion on the AMS 5749 bars appeared to be limited to the saddle area where a minimal amount of crevice corrosion occurred (see Figure 6).

For a detailed examination of the corrosion damage, scanning electron microscopy was employed. Typical corrosion areas are shown in Figures 7 through 9. In general, there was no significant difference between the corrosion in the crevice areas and that on the exposed surfaces for M50 and 52100. Differences were noted between the appearance of the AISI M50 and the AISI 52100. The corrosion on AISI 52100 appeared to cover more surface area, but the corrosion pits on the AISI M50 bars seemed to be deeper. This is not readily apparent in Figures 7 and 8, although sectioning of test bars of both materials through typical corrosion pits provided a clear distinction.

Optical photomicrographs of the sections through the pits are shown in Figures 10 and 11. The greater depths of the AISI M50 corrosion pits are apparent by comparing these photos. This observation agrees with those of Reference 14 which discusses this effect in bearings removed from service.

Corrosion pitting on the AMS 5749 was limited in area and only in the crevice area near the edge of the saddle. These few pits were very shallow, as shown in Figure 12.

The pits shown in Figures 10 through 12 are typical of the deepest pits observed in each material. These pits had depths of approximately 120, 70, and 20 μm (0.005, 0.003, and 0.0008 inch) in the AISI M50, AISI 52100, and AMS 5749, respectively. Pits in a bearing raceway surface are detrimental, because they are likely initiation sites for rolling-element fatigue cracks and subsequent spalling. Thus, the corrosion observed in these specimens would tend to reduce rolling-element fatigue life in AISI M50 more than in either AISI 52100 or AMS 5749.

Corrosion tests identical to those described for the standard through-hardened AMS 5749 were performed on the low carbon and low carbon, nickel added versions of this material (see Sections 3.2 and 3.3). The results were essentially the same in that the modified AMS 5749 exhibited the same excellent corrosion resistance as did the nonmodified high-carbon material.

ORIGINAL PAGE IS
OF POOR QUALITY

4X

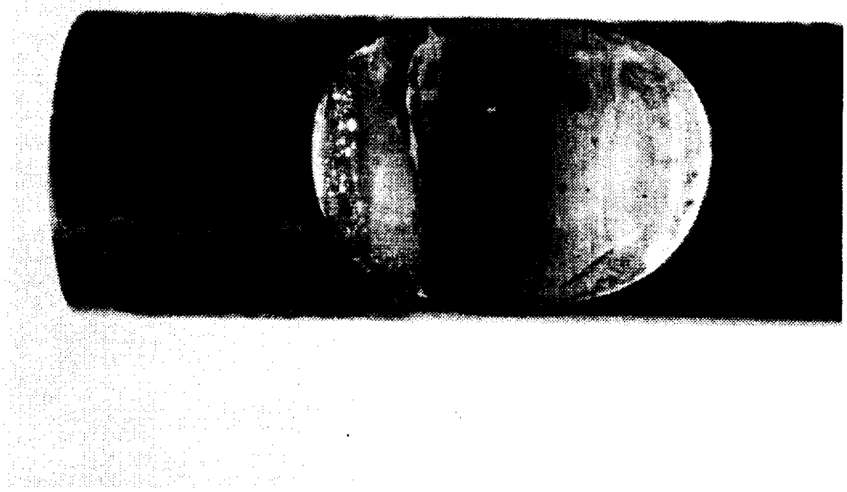

4X

Figure 4. AISI 52100 Test Bars After Corrosion Test.

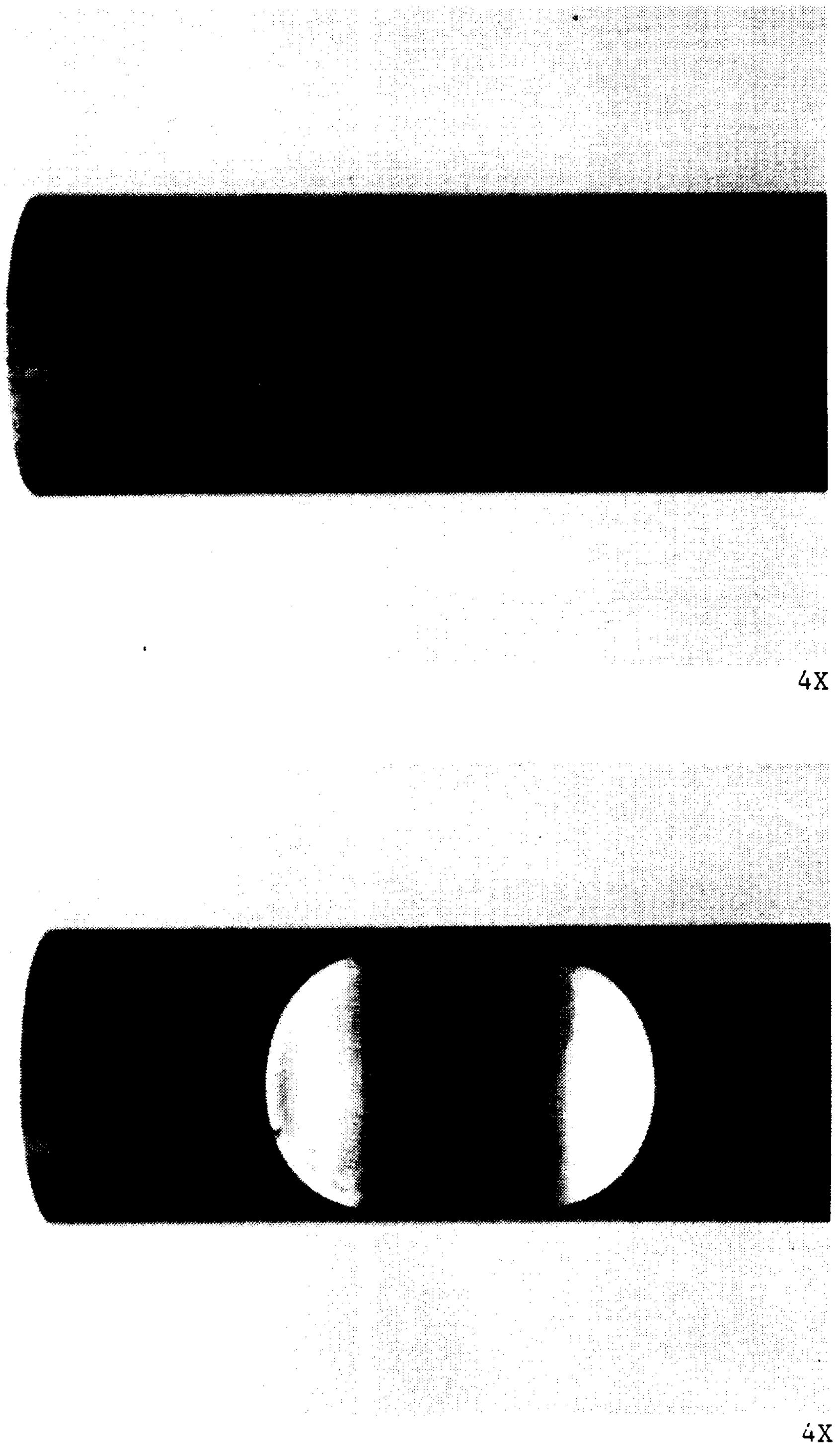

Figure 5. AISI M50 Test Bars After Corrosion Test.

ORIGINAL PAGE IS
OF POOR QUALITY

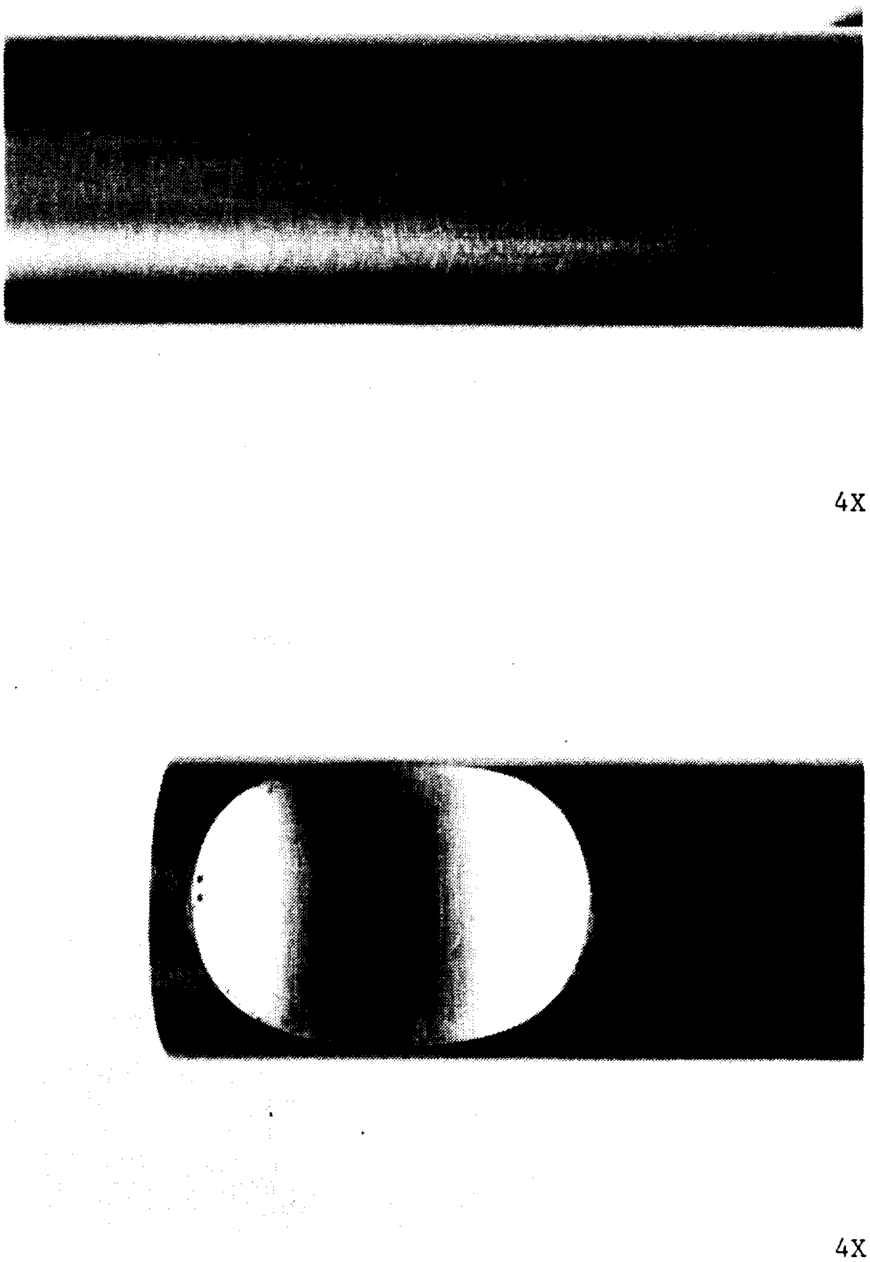

Figure 6. AMS 5749 Test Bars After Corrosion Test.

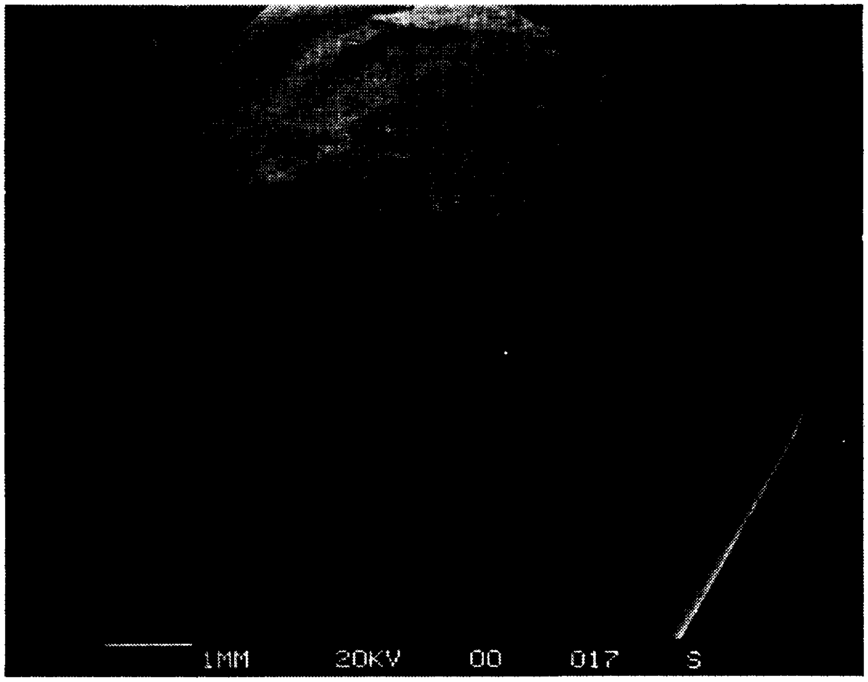

12X

Figure 7. SEM Photograph of 52100 Test Bar After Corrosion Test.

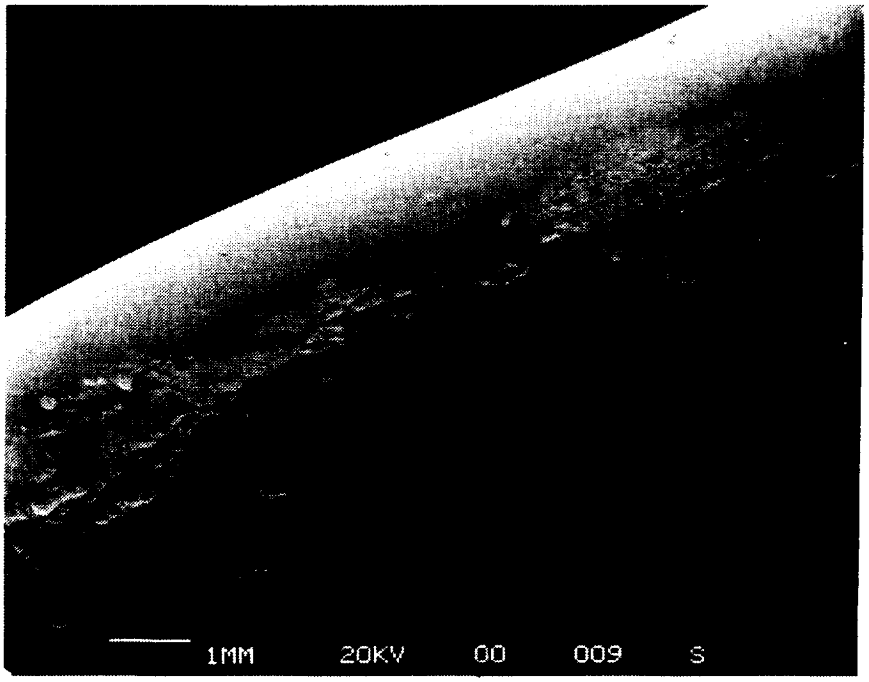

12X

Figure 8. SEM Photograph of M50 Test Bar After Corrosion Test.

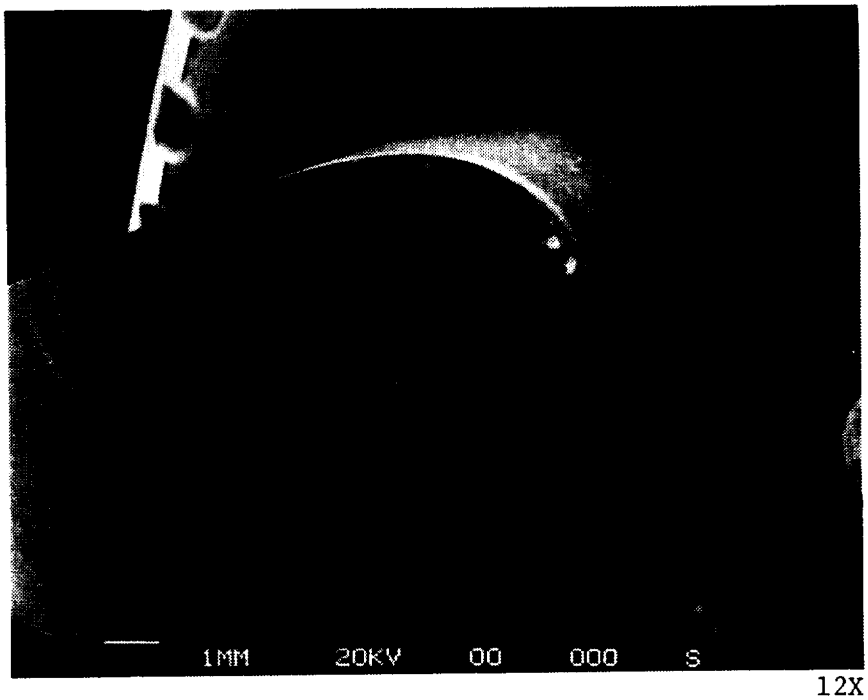

12X

Figure 9. SEM Photograph of AMS 5749 Test Bar After Corrosion Test.

ORIGINAL PAGE IS
OF POOR QUALITY

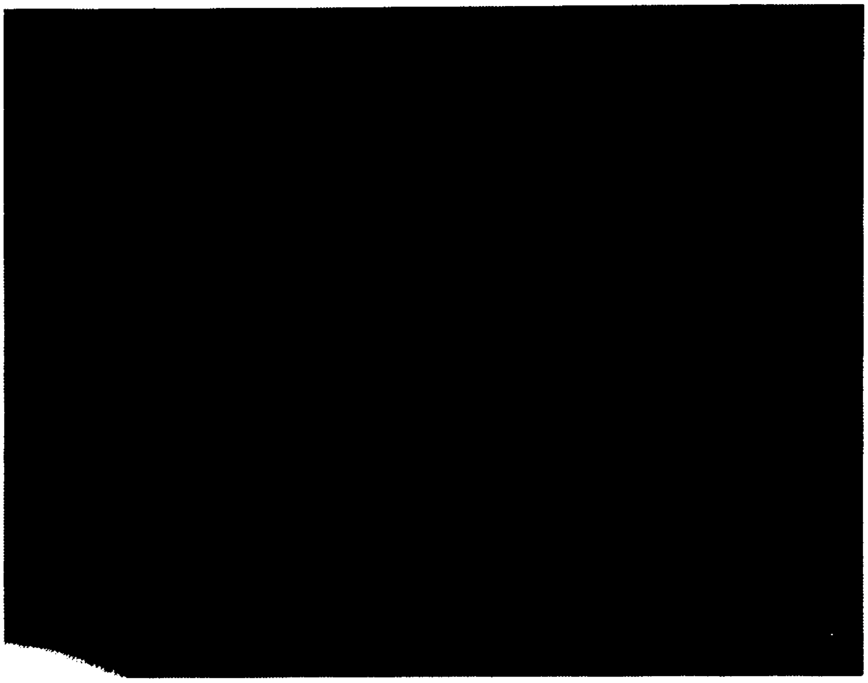
200X


200X

Figure 10. Cross Section Through Typical Corrosion Pits on 52100.

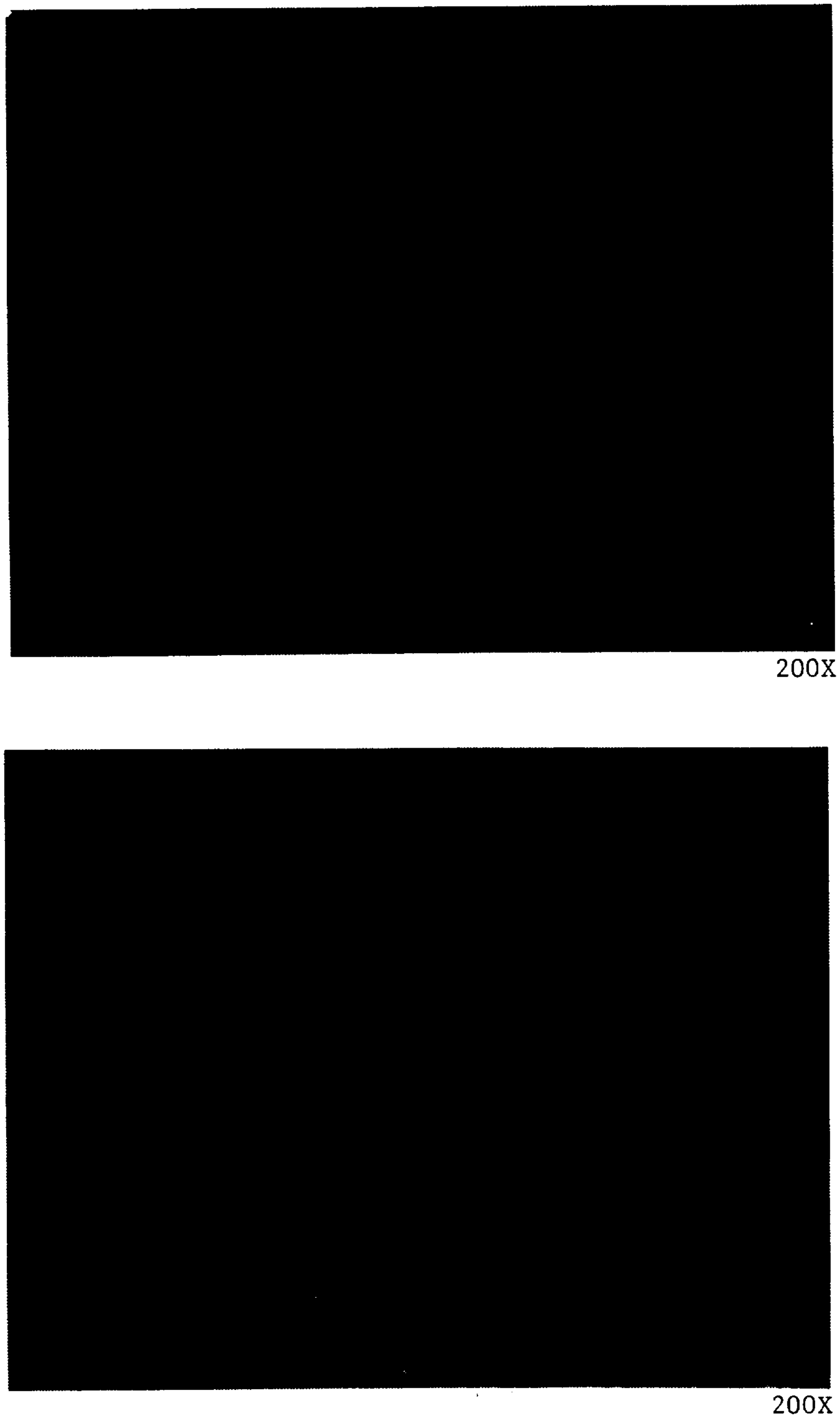

200X

200X

Figure 11. Cross Section Through Typical Corrosion Pits on M50.

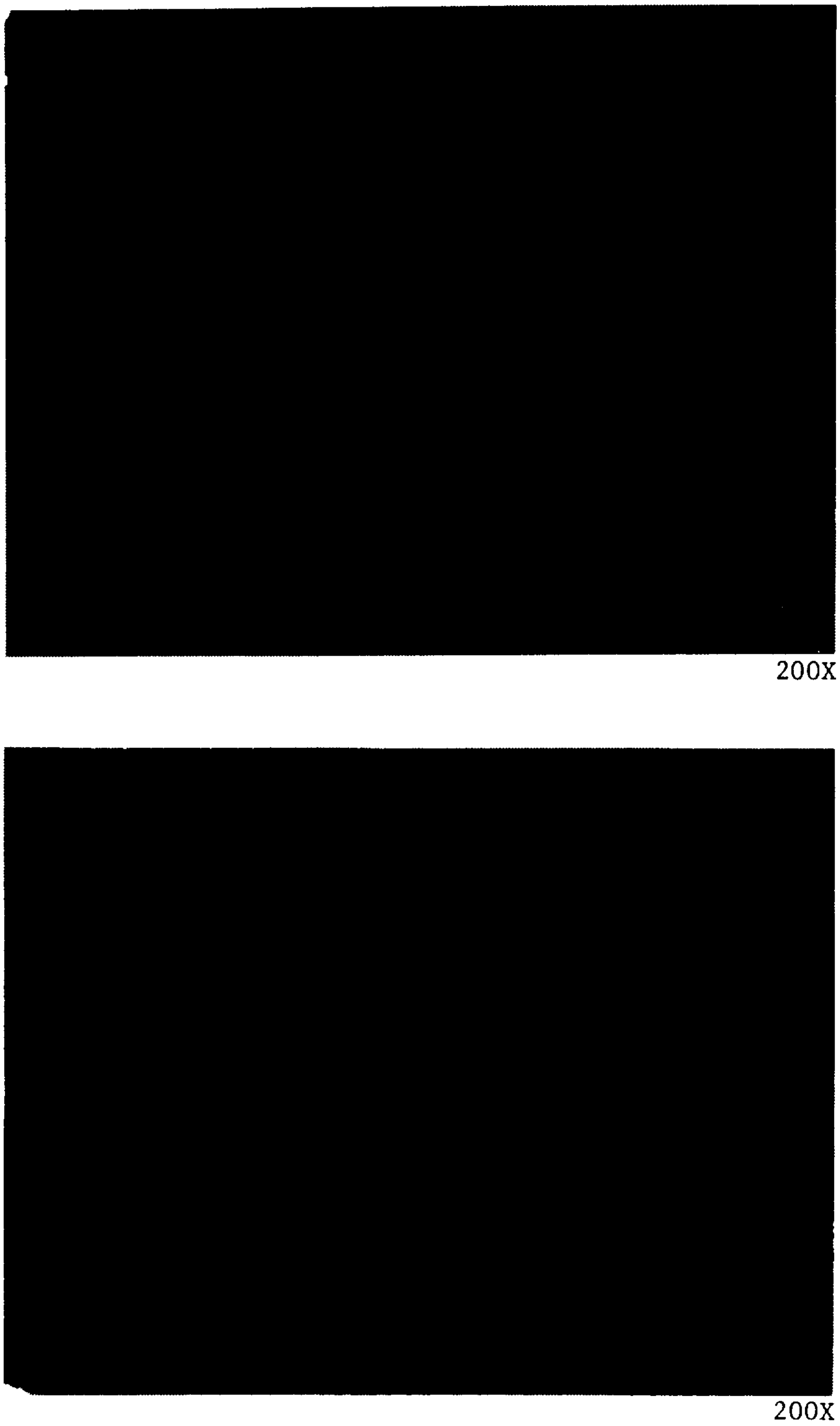

Figure 12. Cross Section Through AMS 5749 Corrosion Test Bar (Note Absence of Corrosion Damage).

A third corrosion test series was performed later in the program when the lower Cr experimental alloys were being evaluated. The results of those tests are discussed in Section 3.4.

3.2 MODIFIED AMS 5749

The original intent of the program was to evaluate a low carbon version of AMS 5749 with the objective of achieving a corrosion resistant carburizing grade bearing alloy. Working with the Latrobe Steel Co., a low carbon AMS 5749 laboratory size [139 mm (5.5 inch) diameter by 457 mm (18 inch) long] ingot was double vacuum melted (VIM-VAR). This ingot had the following chemical composition compared with the standard AMS 5749:

	C	Mn	Si	Cr	Mo	V	S	P
Low Carbon 5749	0.10	0.33	0.30	14.48	3.95	1.17	0.004	0.003
Std 5749	1.15	0.50	0.30	14.50	4.00	1.20	---	---

The ingot was reduced to 70 mm (2.75 inch) round corner square bar, as well as 13 mm (0.5 inch) diameter rod.

A number of trial carburizing and heat treat studies were performed on this material using both gas and vacuum carburizing. None of these treatments resulted in acceptable case microstructures or case hardness levels. Massive amounts of retained austenite were encountered which could not be reduced to an acceptable level and precluded achieving a realistic case hardness (>R_c 58). In addition, excessive grain growth was observed in the low carbon core.

In view of the inability to properly carburize the low carbon AMS 5749, it was decided to further modify the chemistry by incorporating a small amount (~3% by weight) of nickel. The addition of this element successfully worked in the modification of AISI M50, where it acted to repress the retained austenite formation. This was done, and the results of this modification are discussed in Section 3.3.

3.3 LOW CARBON, NICKEL MODIFIED AMS 5749

The inability to achieve a minimum case hardness of R_c 58, a reasonable core hardness (~R_c 40) or an acceptable microstructure with the low carbon version of AMS 5749, led to further alloy modifications in an attempt to achieve the above. Working with the Latrobe Steel Co., four laboratory size heats [29.5 kg (~65 lb)] containing 3% nickel were melted. The nickel was added for austenite stabilization and to reduce the high levels of retained austenite noted in the low carbon AMS 5749. The specific chemical analysis of the four heats is given in Table 3. The carbon levels were varied from 0.1% to 0.3% to permit evaluation of the effect of this on core hardenability.

Table 3. Chemical Analysis of Low Carbon, Nickel Added AMS 5749.

Lab Heat No.	C	Mn	Si	Ni	Cr	Mo	V	S	F
Y66	0.130	0.33	0.32	3.05	14.32	3.75	1.39	0.006	ND*
Y67	0.208	0.34	0.35	3.12	14.42	3.62	1.26	0.005	ND
Y69	0.205	0.25	0.28	3.20	14.65	3.98	1.22	0.005	ND
Y70	0.313	0.25	0.24	3.11	14.61	3.48	1.22	0.005	ND

*(ND = None Detected) *Used for Evaluation

A series of heat treat studies were performed initially to establish the core hardenability with the three carbon levels. Specifically, the 0.1 and 0.3 carbon levels were evaluated. Hardness as a function of austenization and tempering temperature was determined; the results are given in Figures 13 and 14. The effect of austenitizing temperature on the hardness response of the 0.1% carbon material was considerably less than that for the 0.3% carbon material. Varying the tempering temperature between 589 K and 811 K (600° and 1000° F) did not appear to have a significant effect on either material. Typical microstructures of the 0.1%, 0.2%, and 0.3% carbon materials are shown in Figures 15 and 16. As expected, the percentage of ferrite decreases with increasing carbon level. A preliminary carburizing study using the 0.1% carbon material showed a significant increase in ability to diffuse carbon when compared to the non-nickel, modified low carbon material. This is shown in Figure 17, which presents the results of carbon analysis on the two materials after a carburizing cycle.

Short-rod fracture toughness tests were performed on the core of the 0.2% and 0.3% carbon, nickel modified materials; the results of these showed that the fracture toughness was well above the desired 33 Mpa · m ½ (30 ksi · $\sqrt{\text{in.}}$) range. The specific values were:

Carbon content	MPa · $\sqrt{\text{m}}$	K_{IC} (ksi ·$\sqrt{\text{in.}}$)
0.205	61, 55	55.0, 50.2
0.313	48, 40	43.7, 36.5

Retained austenite measurements were also made on several bars (0.1% carbon level) carburized for rather lengthy periods of time (48 and 72 hours). The results shown in Figure 18, indicated that a relatively low retained austenite content could be attained with the nickel modified material.

Austenitizing Temperature	Tempering Temperature				
	589K (600° F)	644K (700° F)	700K (800° F)	755K (900° F)	811K (1000° F)
1255K (1800° F)	26.8*	27.3	27.8	27.3	27.1
1310K (1900° F)	27.9	28.3	28.9	29.1	28.5
1366K (2000° F)	29.0	29.6	31.3	31.7	29.6
1394K (2050° F)	29.5	30.0	30.6	31.3	30.2

* Hardness In Rockwell C

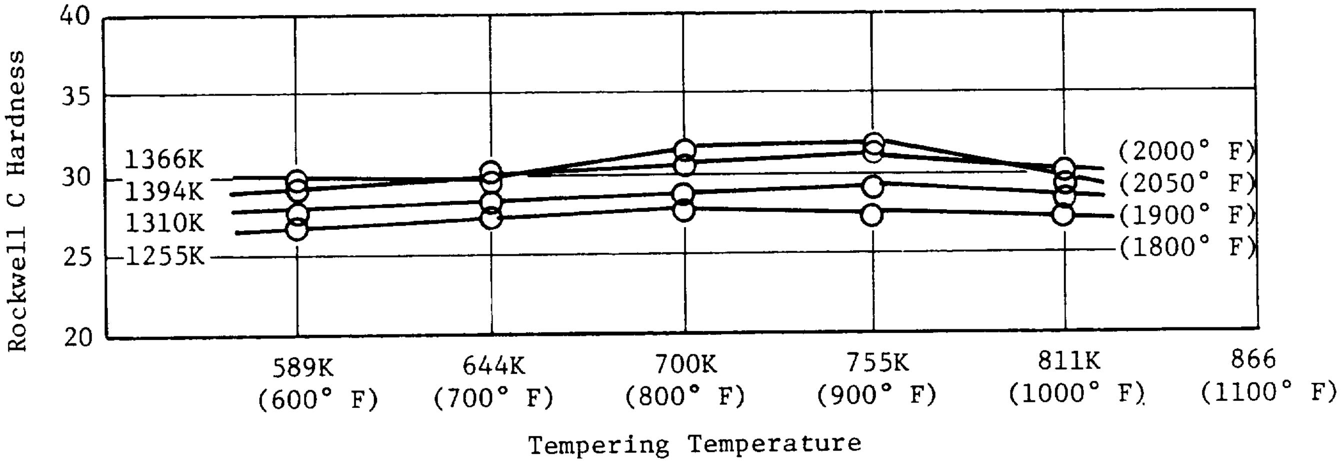

Figure 13. Hardness Versus Tempering Temperature for Low Carbon AMS 5749 + Nickel Austenitized at Various Temperatures: Carbon Content 0.13% (Heat Y66).

Tempering Temperature

Austenitizing Temperature, ° F	As Quenched	589K (600° F)	644K (700° F)	700K (800° F)	755K (900° F)	795K (975° F)	811K (1000° F)
1255K (1800° F)	36.0*	36.8	35.9	36.2	36.5	--	35.1
1310K (1900° F)	41.8	40.8	41.4	42.6	42.8	--	40.1
1366K (2000° F)	43.7	41.8	42.5	43.8	43.9	--	41.5
1394K (2050° F)	46.5	42.9	43.0	44.7	45.7	46.9	43.9
1422K (2100° F)	49.6	46.4	47.4	48.2	49.0	--	46.1

* Hardness in Rockwell C

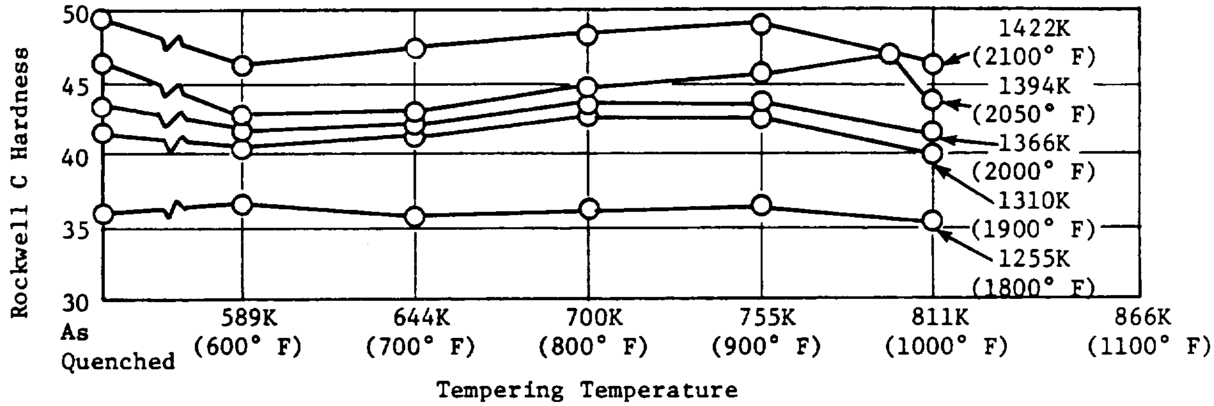

Figure 14. Hardness Versus Tempering Temperature for Low Carbon AMS 5749 + Nickel Austenitized at Various Temperatures: Carbon Content 0.313% (Heat Y70).

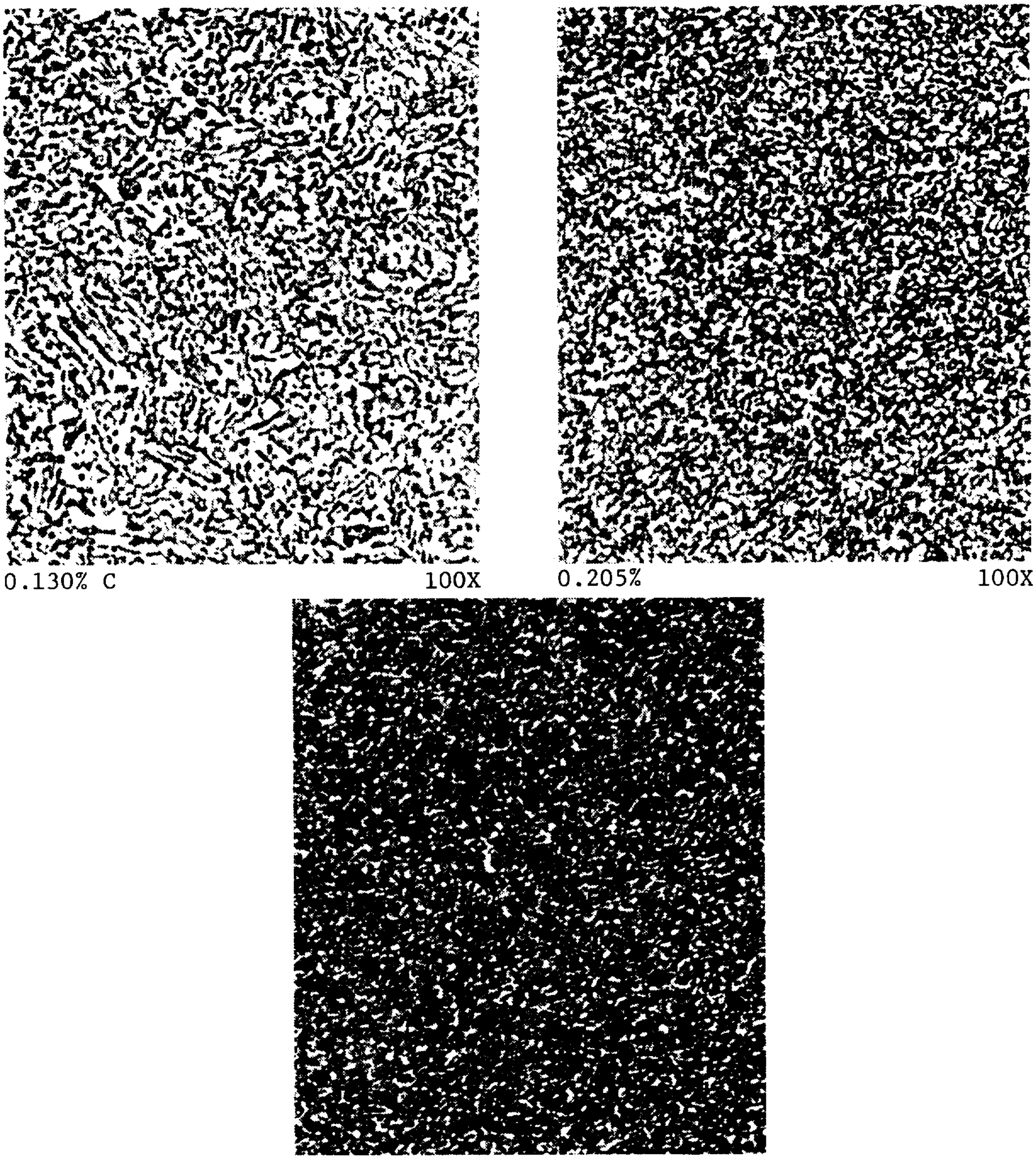

0.130% C 100X

0.205% 100X

0.313% 100X

Figure 15. Typical Microstructure Low Carbon + Nickel Added AMS 5749; Austenitized at 1394 K (2050° F); Oil Quenched; Subzero/ Cool at 200 K (-100° F); Double Temper 2+2 Hours at 797 K (975° F); Etchant, 3% Nital.

0.130% C 500X

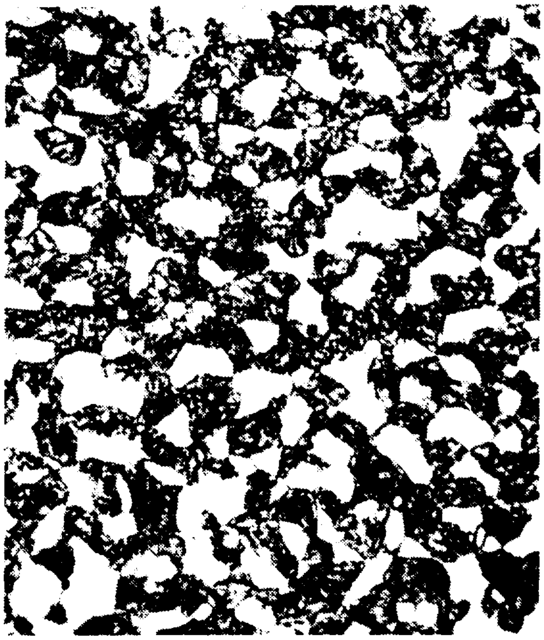

0.205% 500X

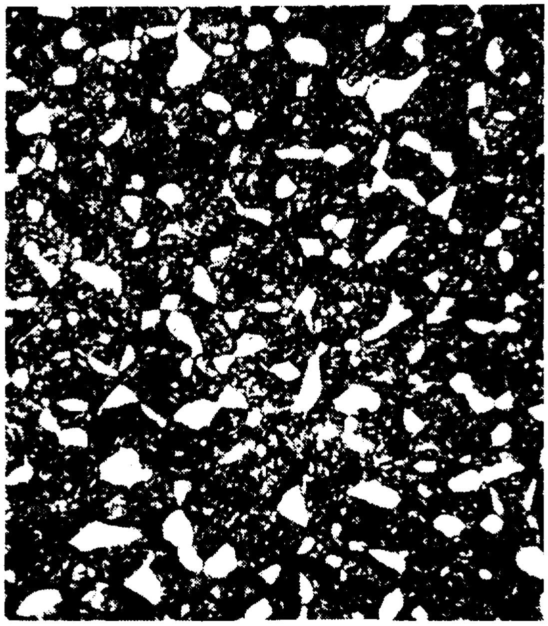

0.313% 500X

Figure 16. Typical Microstructure Low Carbon + Nickel Added AMS 5749; Austenitized at 1394 K (2050° F); Oil Quenched; Subzero/ Cool at 200 K (-100° F); Double Temper 2+2 Hours at 797 K (975° F); Etchant, 3% Nital.

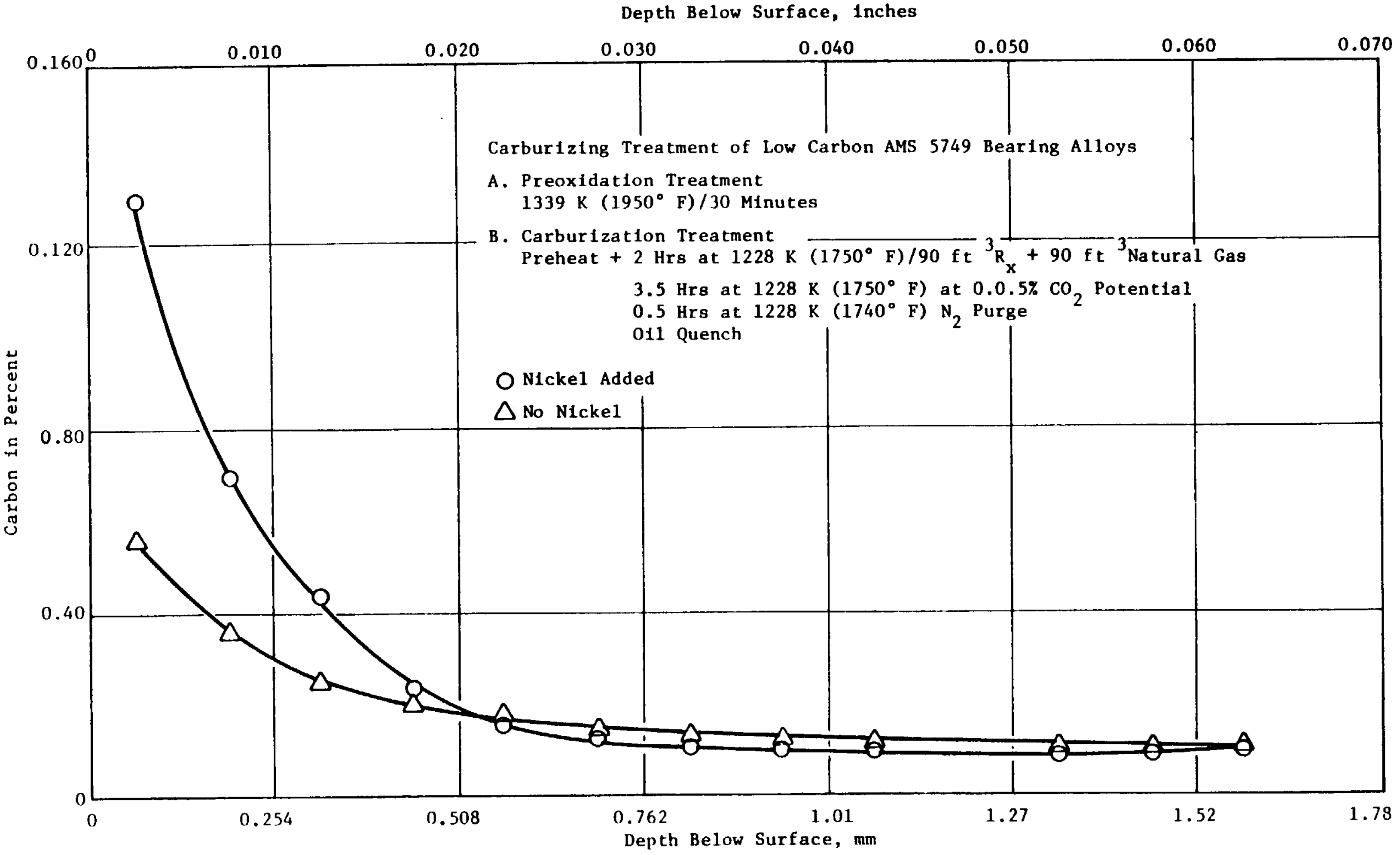

Figure 17. Carburizing Characteristics of Low Carbon AMS 5749 Bearing Alloys.

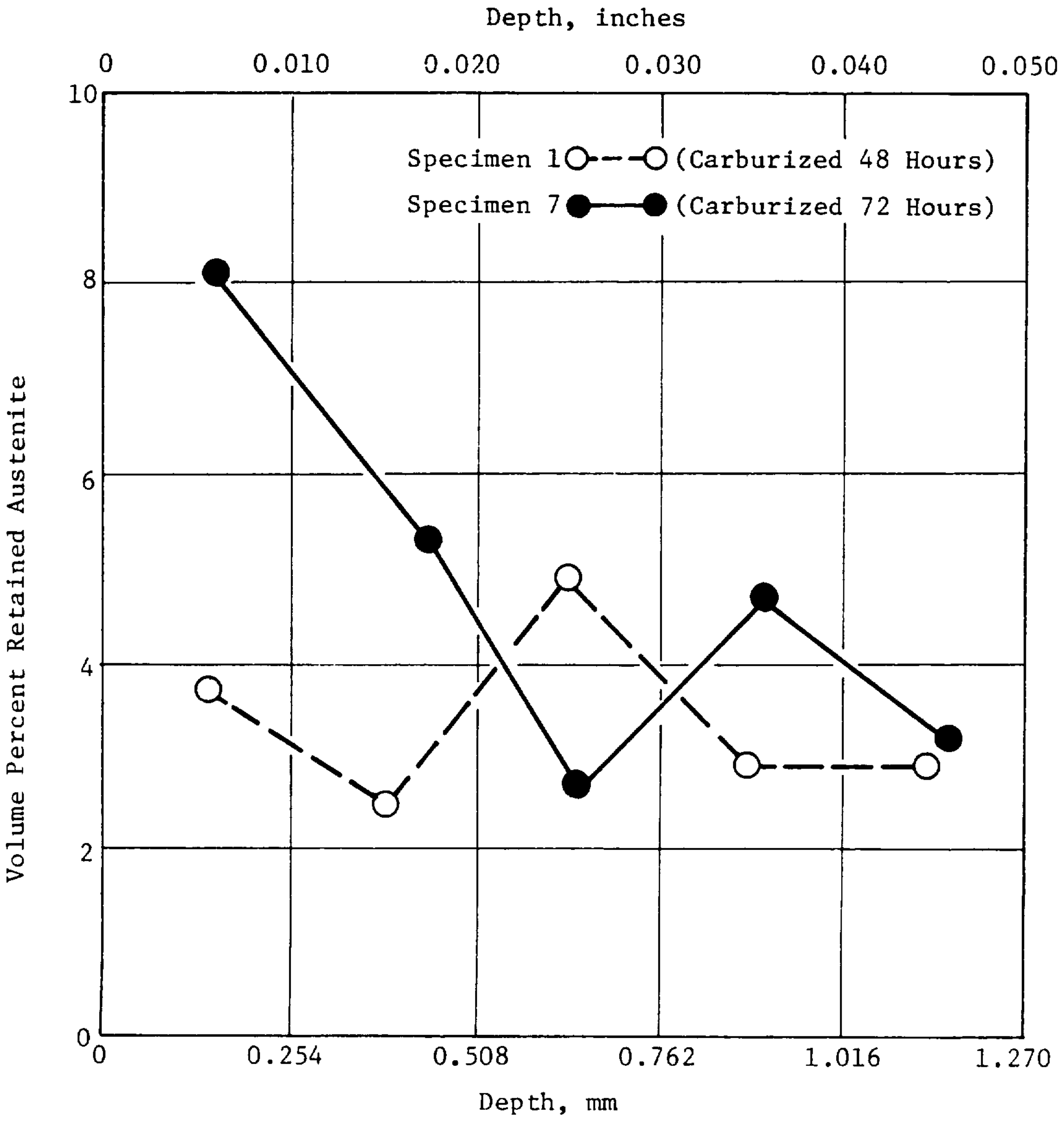

Figure 18. Subsurface Volume Percent Retained Austenite Distribution, Carburized Nickel Modified Low Carbon AMS 5749.

In view of these initial encouraging results, a comprehensive evaluation program was started to establish a viable carburization cycle for this material. A total of 184 carburizing and heat treat cycles were performed. The results of these were evaluated using metallographic and microhardness measurements techniques as well as carbon analysis. None of these resulted in what was considered an adequate combination of case and core structure and hardness. Consequently, it is not considered useful or beneficial to review all of these in detail. Therefore, in the following section an overview is given to indicate representative structures and hardness ranges encountered during this evaluation.

The three carbon levels given in Table 3 were evaluated. As a point of reference, Figure 19 shows the microstructure of standard AMS 5749, heat-treated as indicated to provide a hardness of R_c 61. The structure is characterized by a martensitic matrix with large insoluble carbides. By contrast, Figures 20 through 22 show the microstructure of similarly hardened nickel modified, low carbon AMS 5749. The structure is a combination of low carbon martensite and ferrite, ranging in hardness from R_c 35 for the 0.1% carbon material to R_c 42 for the 0.3% carbon material.

Using the carburizing cycle shown in Table 4, a case hardness in excess of R_c 65 could be achieved in the nickel modified, low carbon AMS 5749 (Table 5). Predictably, the structure of the case showed the massive carbide agglomeration illustrated in Figure 23 and considered totally unsuitable for a bearing application. This massive carbide formation was encountered regardless of carburizing temperatures [1172 K to 1228 K (1650° to 1750° F)] when the parts were slow cooled after carburizing. Oil quenching after carburization reduced the carbide mass but also tended to lower the case hardness to around R_c 56 to 58, with a core hardness of about R_c 30 to 33. Table 6 is another typical carburizing cycle used in this phase of the evaluation. A typical case structure for oil-quenched samples is shown in Figure 24 with matching hardness profiles given in Table 7.

Earlier carburizing trials had been made using lower carbon potentials (~0.5 to 0.6%) in order to reduce the rapid and massive buildup of carbide. These attempts, while achieving a smaller carbide mass, failed to generate adequate hardness levels. However, because of the inability to achieve a desirable case-core structure and hardness combination using the higher carbon potentials, it was decided to try to establish the best possible combination which could be achieved at this time. The microstructures in Figures 25 through 33 illustrate the results of this study. As can be seen, the case structures were greatly improved over those generated with the higher carbon potential levels, although hardness still peaked at or near R_c 58. Generally, the core structure was a rather even mix of martensite and ferrite which, according to Reference 15, would impair fracture toughness. It was notable that in some samples the case structures showed a carbide morphology superior to that seen in the standard, through hardened AMS 5749. In particular, the structure in Figure 26 is cited. In all carburizing cycles represented by this latter series of photomicrographs, a boost-diffuse cycle was used, apparently with good results.

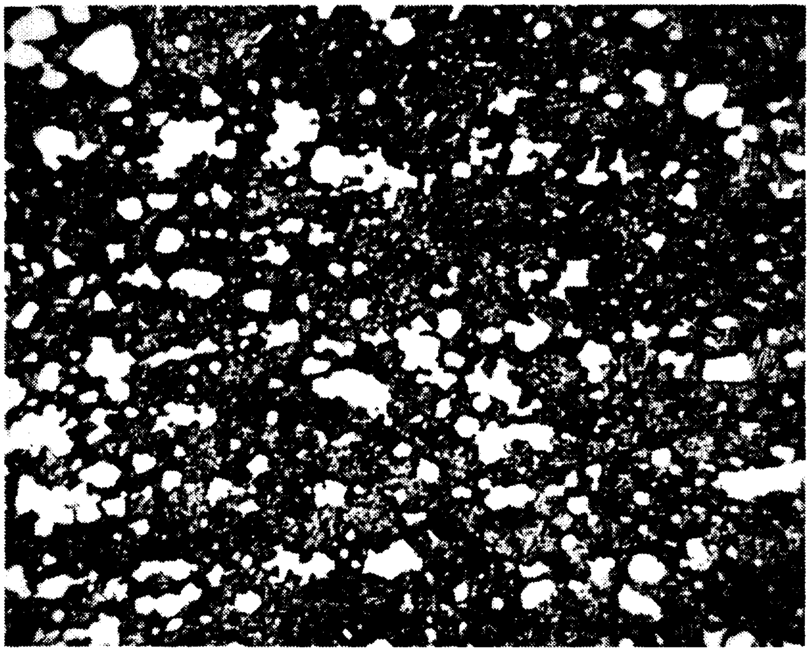

500X

Austenitized at 1339 K (1950° F)
866K (1100° F) Oil Quench
Air Cooled to R.T.
Temper: 755K (900° F)/2 hours
200K (- 100° F)/1 hour
755K (900° F)/2 hours
Hardness: R_c 61
Etchant: Mod. Picral

Figure 19. Microstructure of AMS 5749.

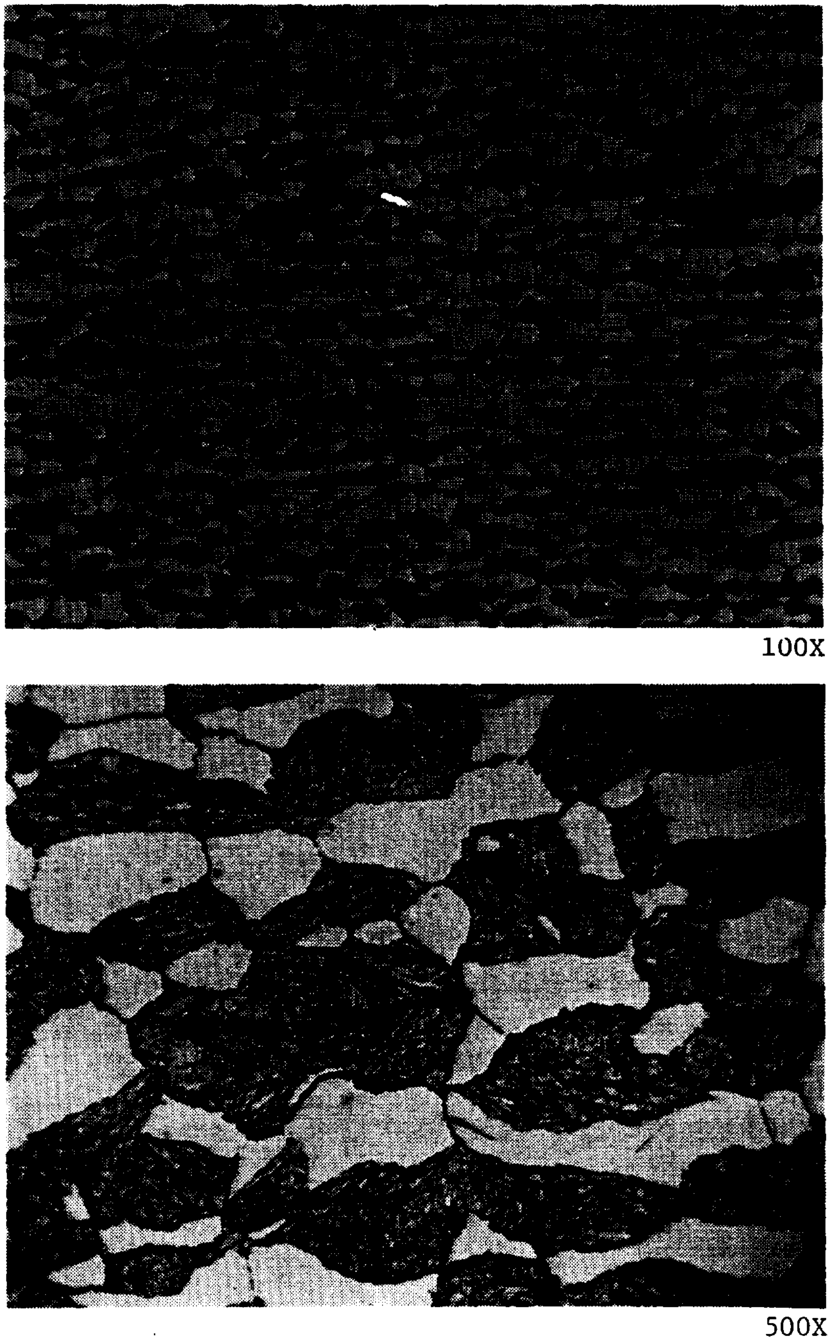

Figure 20. Microstructure of Nickel Modified, Low Carbon (0.13%) AMS 5749: Austenitized at 1366K (2000° F); Temper 811 K (1000° F) 2+2 Hours; Hardness R_c 35; Etchant Mod. Picral.

ORIGINAL PAGE IS
OF POOR QUALITY

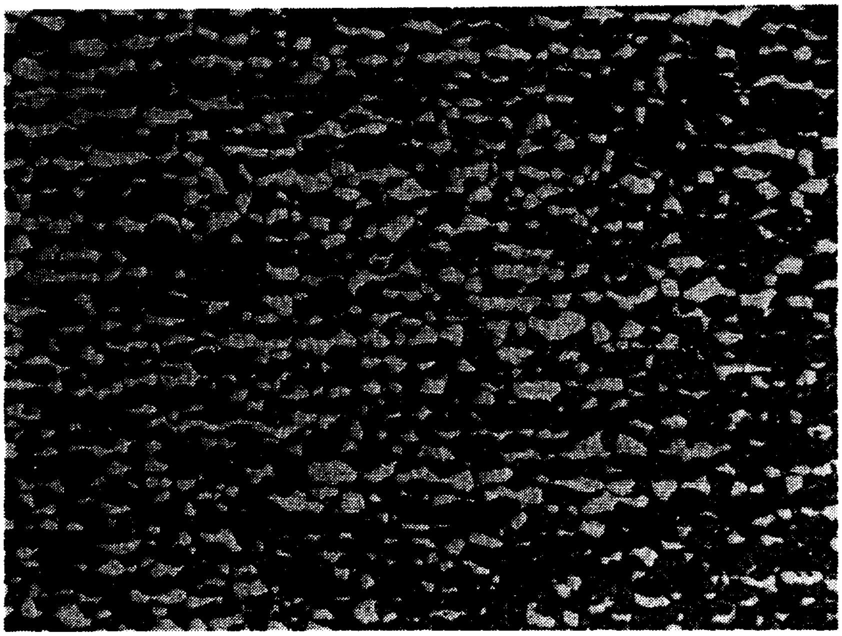

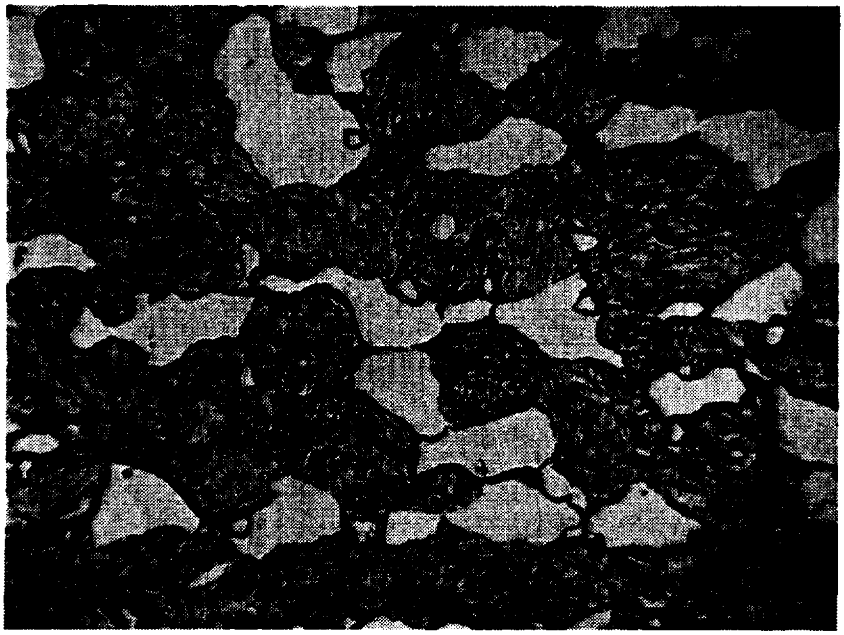

Figure 21. Microstructure of Nickel Modified, Low Carbon (0.208%) AMS 5749: Austenitized at 1366 K (2000° F); Temper 811 K (1000° F) 2+2 Hours; Hardness R_c40; Etchant Mod. Picral.

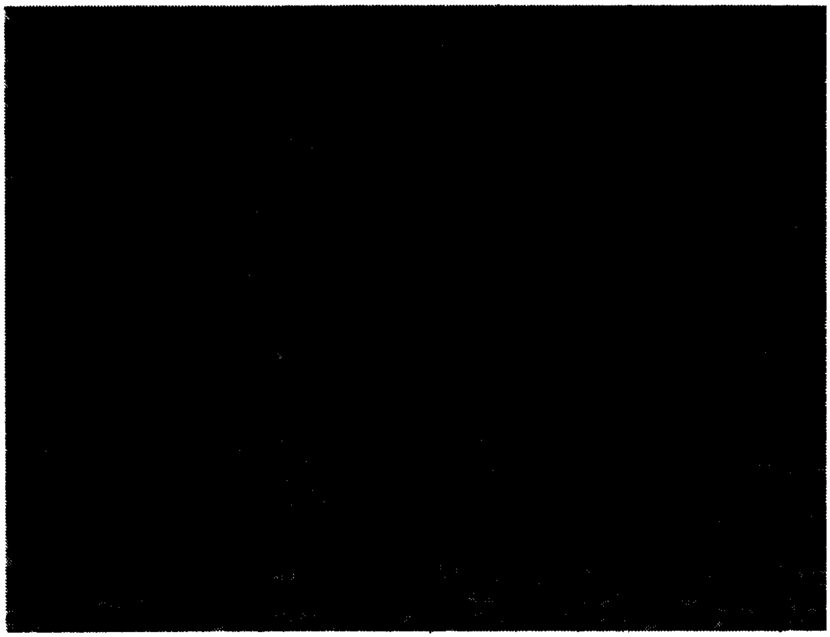

100X

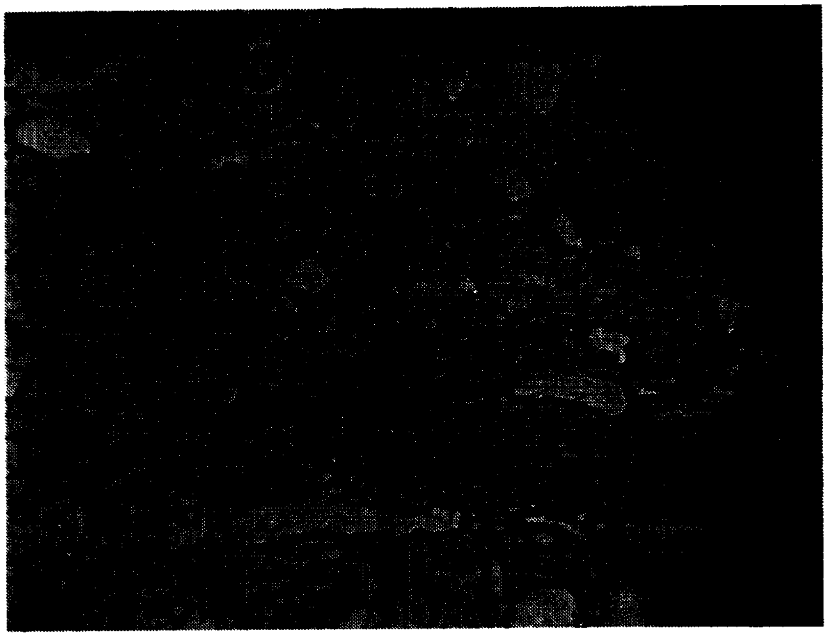

500X

Figure 22. Microstructure of Nickel Modified, Low Carbon (0.313%) AMS 5749: Austenitized at 1366 K (2000° F); Temper 811 K (1000° F) 2+2 Hours; Hardness R_C42; Etchant Mod. Picral.

Table 4. Carburizing and Hardening Cycle for 0.1% Carbon, Nickel Modified AMS 5749.

- Preoxidize: 1228 K (1750° F) for 1 Hour in Air
- Carburize: 1366 K (1700° F) for 12 Hours

  Carbon Potential = 1.0% for 9 Hours,
  0.95% for 3 Hours

  Furnace Cool to 1061 K (1450° F) in 30 Minutes, Air Cool to Room Temperature
- Preheat: 1200 K (1700° F) for 1 Hour
- Austenitize: 1339 K (1950° F) for 5 Minutes in Salt

  Quench into 866 K (1100° F) Salt, Hold for 15 Minutes, Air Cool to Room Temperature
- Temper: 839 K (1050° F) 2 Hours
- Deep Freeze: 200 K (-100° F) 1 Hour
- Temper: 839 K (1050° F) 2 Hours

Table 5. Hardness Profile in Nickel Modified, Low Carbon AMS 5749 Carburized Per Cycle Shown in Table 4.

Depth Below Surface		Hardness
mm	(in.)	R_c*
0.051	0.002	64
0.102	0.004	64
0.152	0.006	67
0.203	0.008	65
0.254	0.010	66
0.381	0.015	63
0.508	0.020	58
0.635	0.025	54
0.762	0.030	52
1.016	0.040	45
1.270	0.050	42
1.524	0.060	38
2.032	0.080	37
2.540	0.100	37

*Converted From 500 Gram Knoop Microhardness

Figure 23. Case Microstructure of Nickel Modified, Low Carbon AMS 5749 After Carburizing According to Table 4.

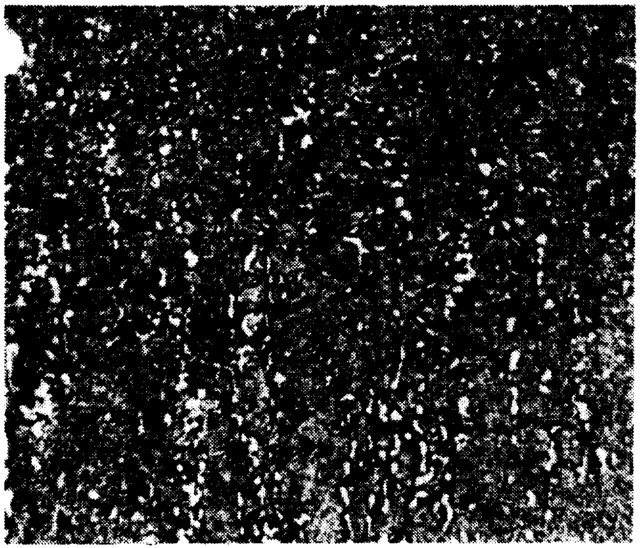

0.10% C 100X

Etchant: Mod. Picral

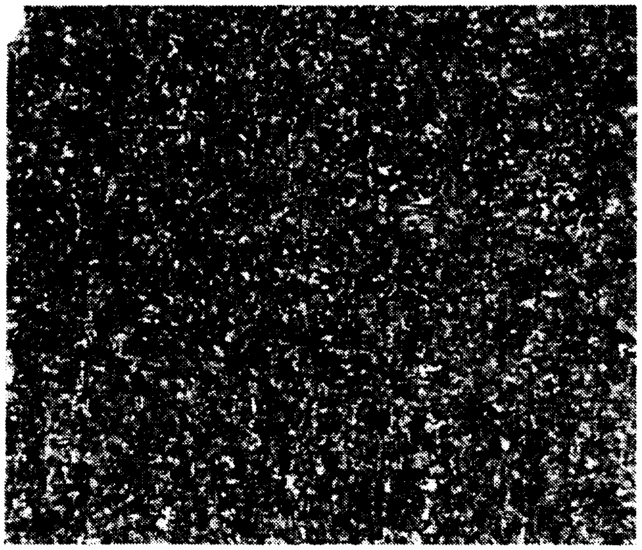

0.20% C 100X

Etchant: Mod. Picral

Figure 24. Typical Case Structure of Nickel Modified, Low Carbon AMS 5749, Carburized Per Cycle Shown in Table 6.

Table 6. Carburizing Cycle for Nickel Modified, Low Carbon AMS 5749 (Oil Quenched).

- **Preoxidize:** 1228 K (1750° F) for 2 Hours in Air
- **Preheated:** 1200 K (1700° F) for 1 Hour
- **Carburized:** 1200 K (1700° F) for 12 Hours
  Carbon Potential = 1% for 9 Hours
  = 0.95% for 3 Hours
  Oil Quench Into 366 K (200° F) Oil
  Air Cool to Room Temperature
- **Preheat:** 1200 K (1770° F) 1 Hour
- **Austenitize:** 1394 K (2050° F) for 15 Minutes
  Furnace Cool to 855 K (1100° F)
  Air Cool to Room Temperature
- **Temper:** 797 K (975° F) for 2 Hours
- **Deep Freeze:** 200 K (-100° F) for 1 Hour
- **Temper:** 797 K (975° F) for 2 Hours

Table 7. Hardness Profile of Nickel Added, Low Carbon AMS 5749 Carburized Per Cycle Shown in Table 6.

Depth Below Surface		0.10 Carbon Hardness	0.20 Carbon Hardness
mm	(in)	Rc*	Rc*
0.051	0.002	55	52
0.102	0.004	57	55
0.152	0.006	56	56
0.203	0.008	56	57
0.254	0.010	57	56
0.381	0.015	56	55
0.508	0.020	55	53
0.635	0.025	55	53
0.762	0.030	53	48
0.889	0.035	48	---
1.016	0.040	39	35
1.270	0.050	32	35
1.524	0.060	34	33
1.778	0.070	33	29
2.032	0.080	30	34
2.286	0.090	32	36
2.540	0.100	32	33

*Converted From 500 Gram Knoop Microhardness

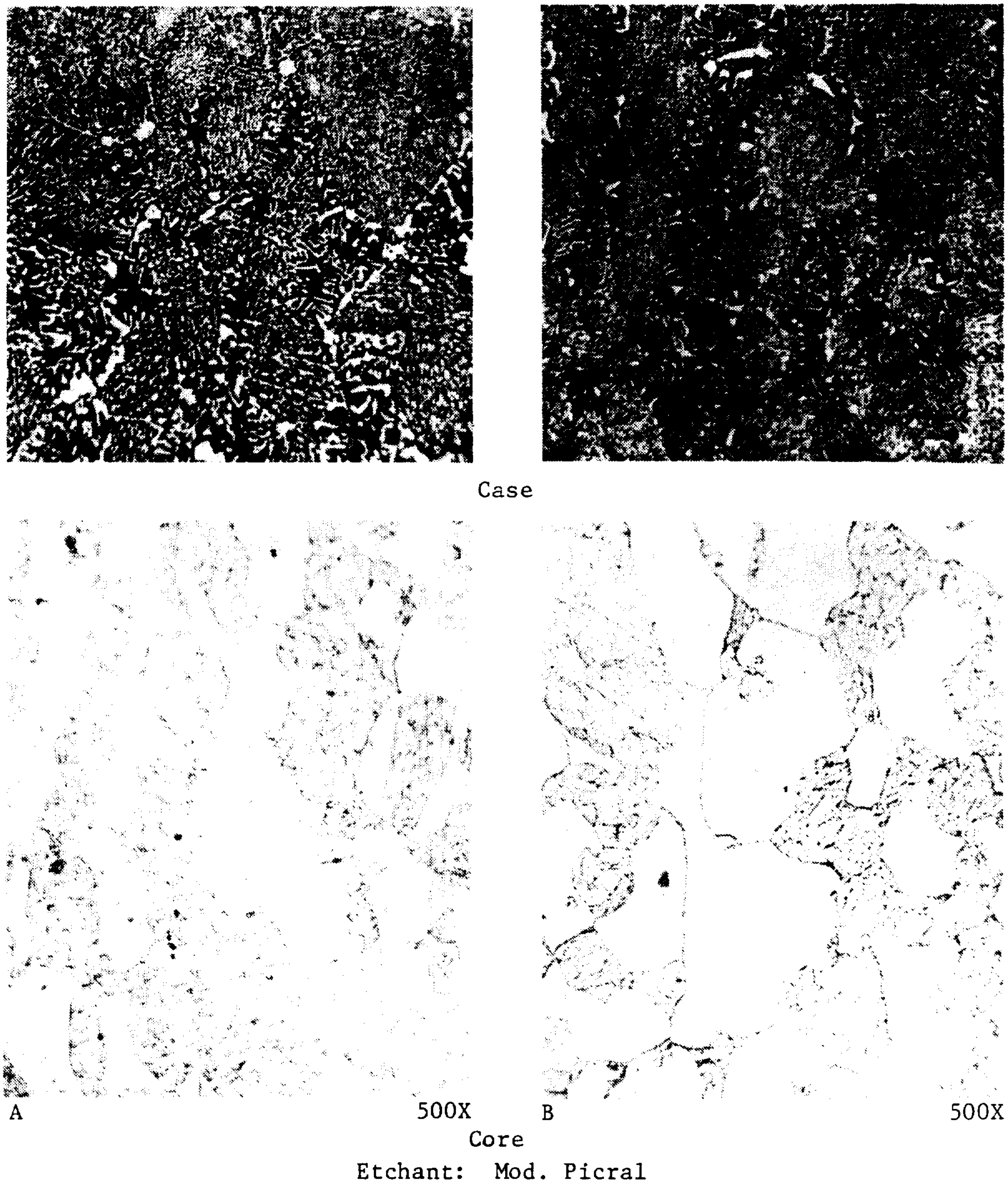

Figure 25. **Structure of Nickel Modified, Low Carbon ANS 5749; A = 0.1% Carbon Carburized at 1200 K (1700° F) 9 Hour CP = 1.0%, 6 Hour CP = 0.7%: B - 0.1% Carbon Carburized at 1200 K (1700° F) 12 Hour CP = 0.7%: A&B Austenitized at 1353 K (1975° F), Tempered at 839 K (1050° F) 2+2 Hours; Etchant Mod. Picral.**

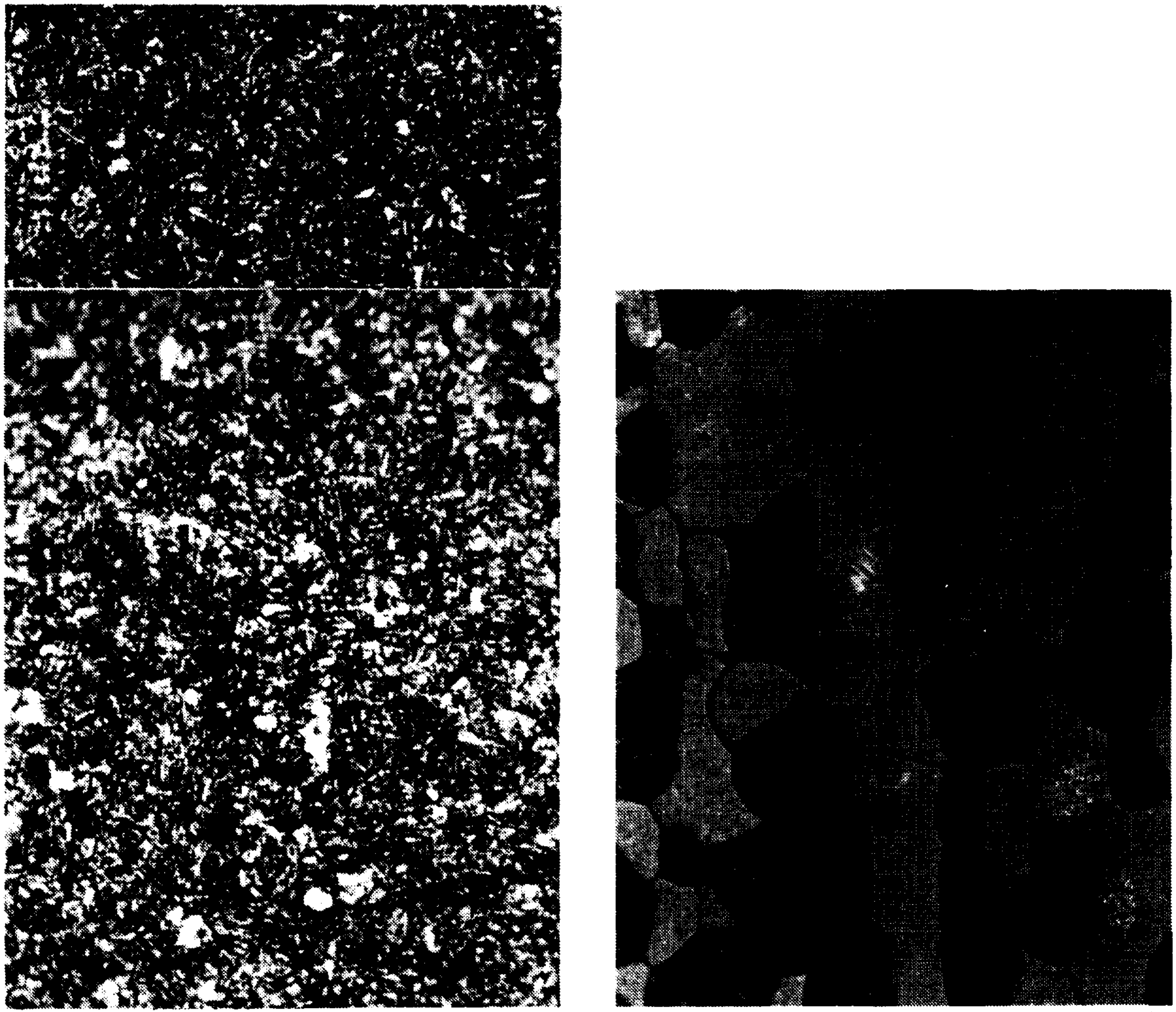

Etchant: Mod. Picral 500X
Case (Hardness = R_c 58)

Etchant: Mod. Picral 500X
Core (Hardness = R_c 36)

Figure 26. Structure of Nickel Modified, Low Carbon (0.1%) AMS 5749: Carburized 48 Hours at 1228 K (1750° F); CP = 0.8% for 6 Hours, 0.5% for 42 Hours; Austenitized at 1339 K (1950° F); Salt Quenched; Tempered 783 K (950° F) 2+2 Hours.

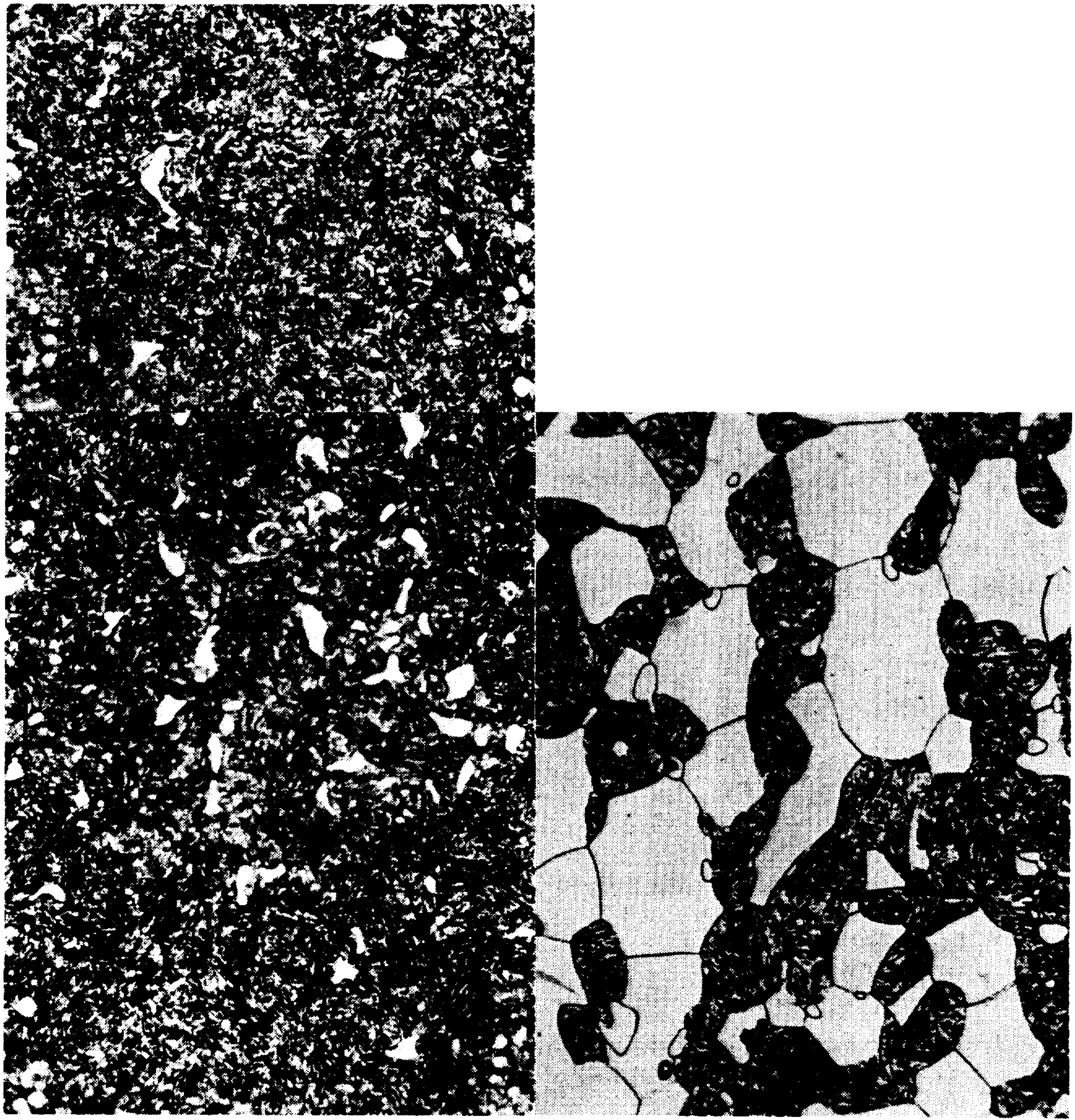

Etchant: Mod. Picral 500X
Case (Hardness = R_c 55)

Etchant: Mod. Picral 500X
Core (Hardness = R_c 36)

Figure 27. Structure of Nickel Modified, Low Carbon (0.2%) AMS 5749: Carburized 48 Hours at 1228 K (1750° F); CP = 0.8% for 6 Hours, 0.5% for 42 Hours; Austenitized at 1339 K (1950° F), Salt Quenched, Tempered 783 K (950° F) 2+2 Hours.

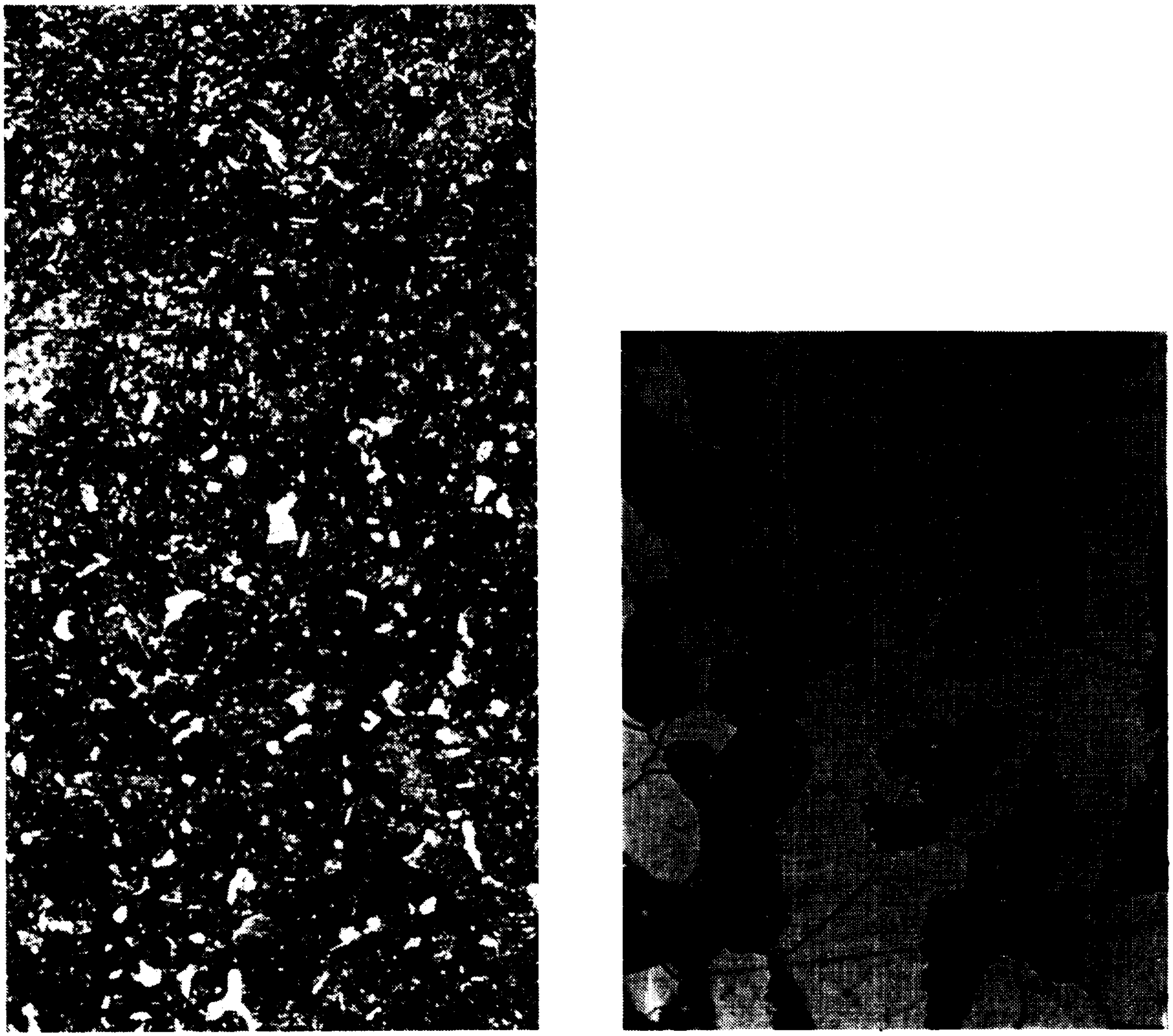

Etchant: Mod. Picral 500X
Case (Hardness = R_C 53)

Etchant: Mod. Picral 500X
Core (Hardness = R_C 36)

Figure 28. Structure of Nickel Modified Low Carbon (0.2%) AMS 5749: Carburized 48 Hours at 1200 K (1700° F); CP = 0.8% for 6 Hours, 0.5% for 42 Hours; Austenitized at 1339 K (1959° F); Oil Quenched, Tempered 783 K (950° F) 2+2 Hours.

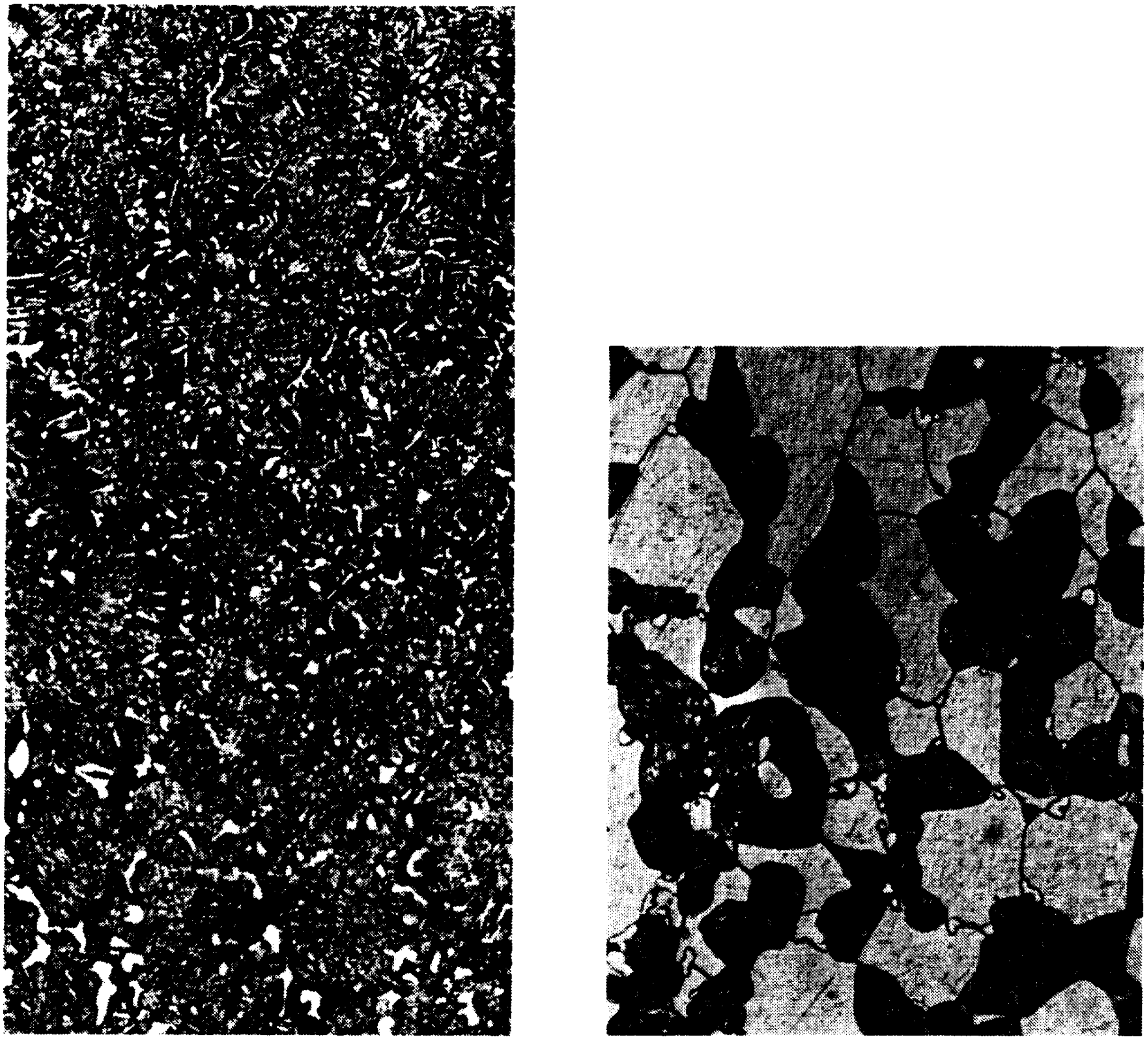

Etchant: Mod. Picral 500X

Case (Hardness = R_C 63)

Etchant: Mod. Picral 500X

Core (Hardness R_C 35)

Figure 29. Structure of Nickel Modified Low Carbon (0.1%) AMS 5749: Carburized 72 Hours at 1228 K (1750° F); CP = 0.8% for 6 Hours, 0.5% for 66 Hours; Austenitized at 1339 K (1950° F); Salt Quenched; Tempered 783 K (950° F) 2+2 Hours.

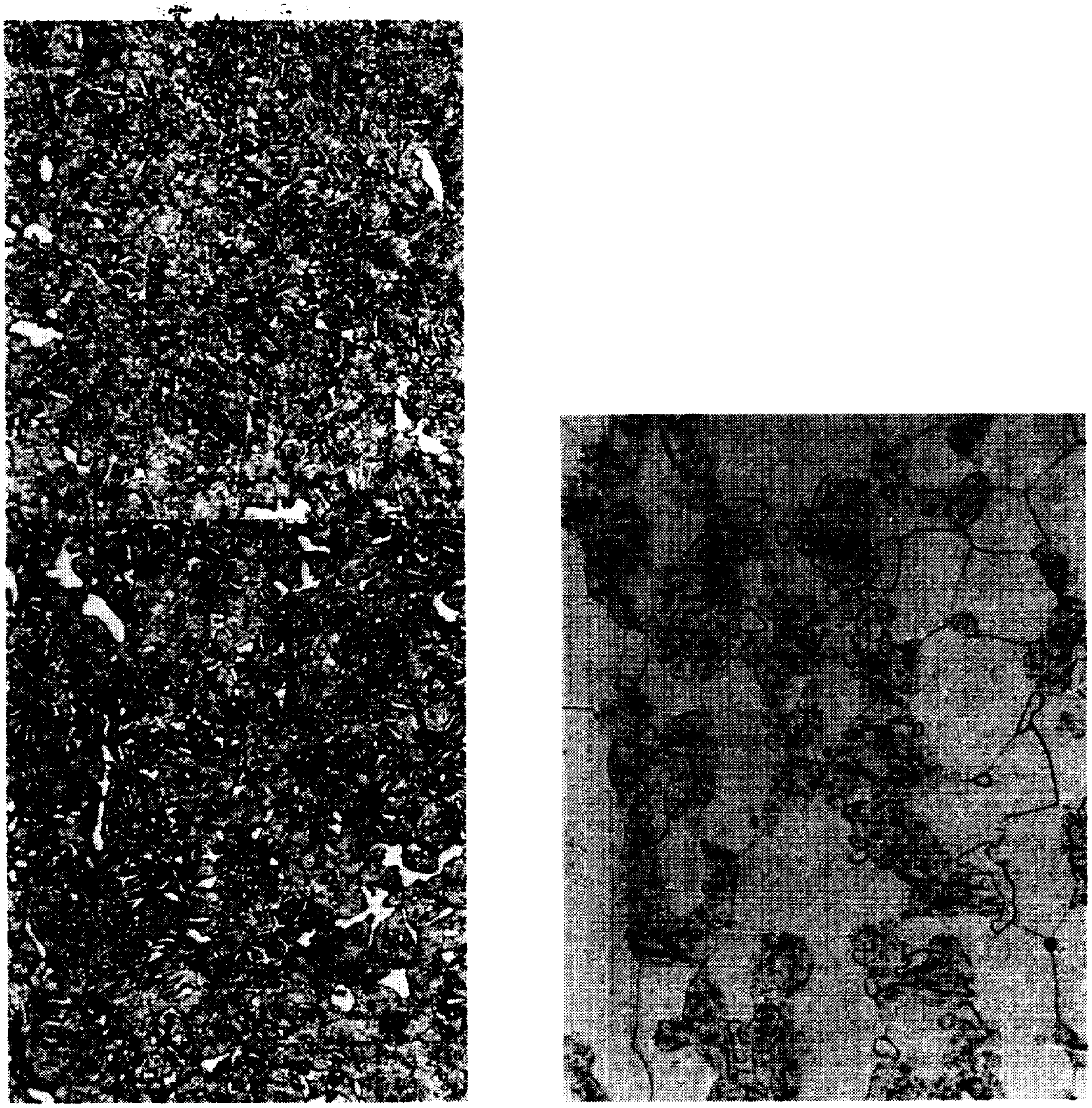

Etchant: Mod. Picral 500X

Case (Hardness = R_C 62)

Etchant: Mod. Picral 500X

Core (Hardness = R_C 37)

Figure 30. Structure of Nickel Modified Low Carbon (0.2%) AMS 5749: Carburized 72 Hours at 1228 K (1750° F); CP = 0.8% for 6 Hours, 0.5% for 66 Hours; Austenitized at 1339 K (1950° F); Oil Quenched; Tempered 783 K (950° F) 2+2 Hours.

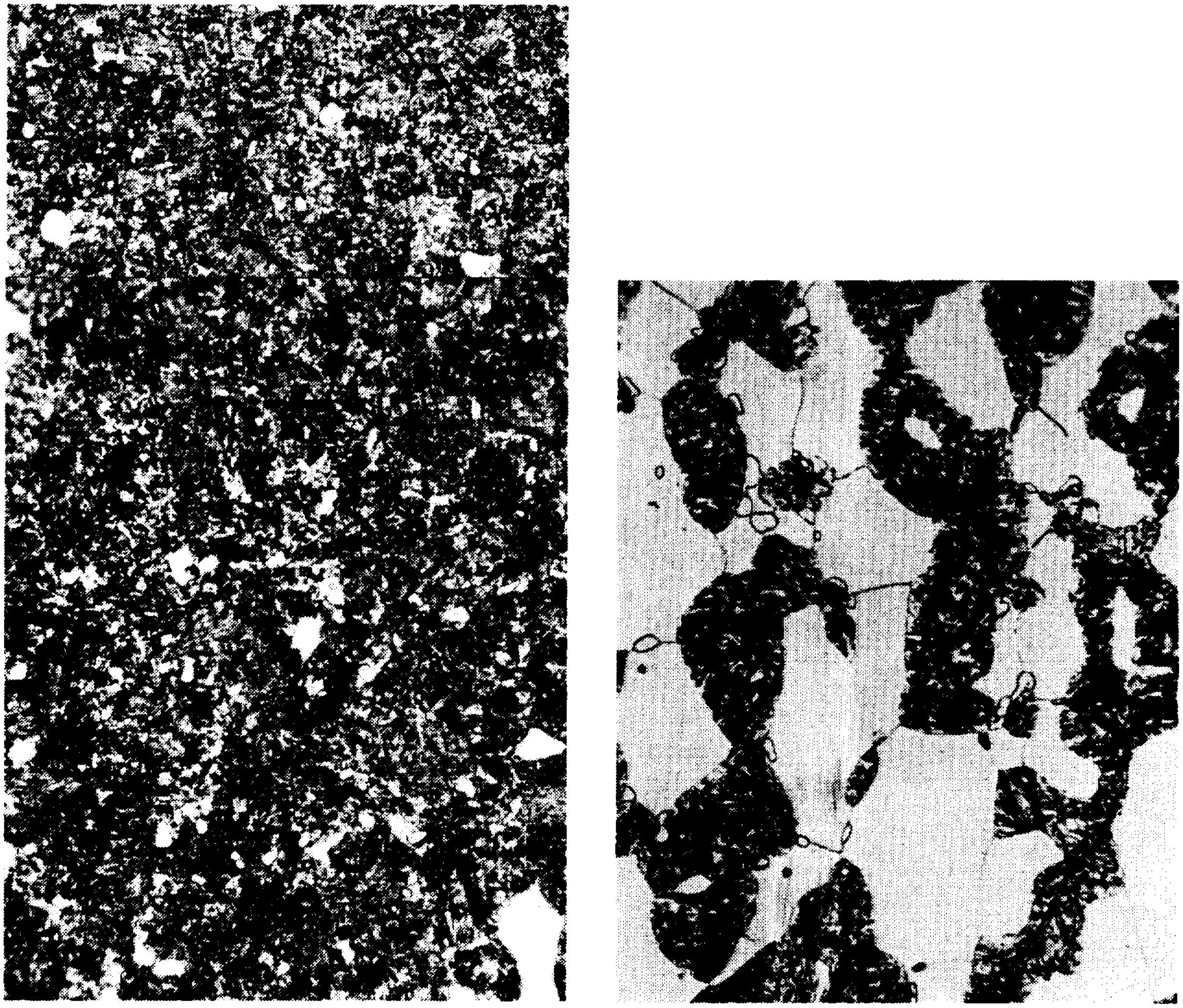

Etchant: Mod. Picral 500X

Case (Hardness = R_c 56)

Etchant: Mod. Picral 500X

Core (Hardness = R_c 34)

Figure 31. Structure of Nickel Modified Low Carbon (0.1%) AMS 5749: Carburized 72 Hours at 1228 K (1750° F); CP = 0.8% for 6 Hours, 0.5% for 66 Hours; Austenitized 1339 K (1950° F); Still-Air Cooled; Tempered 783 K (950° F) 2+2 Hours.

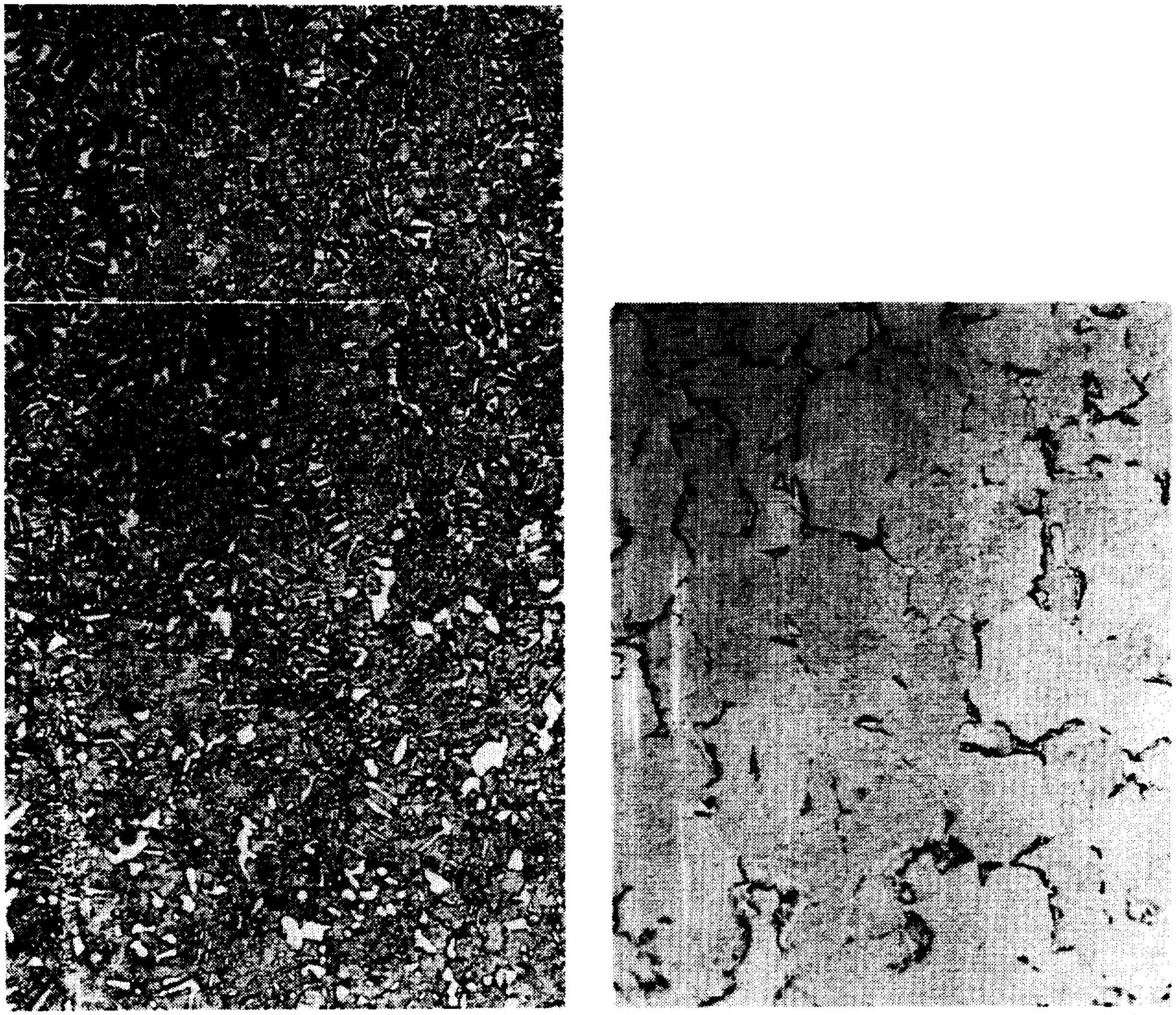

Etchant: Mod. Picral 500X

Case (Hardness = R_c 58)

Etchant: Mod. Picral 500X

Core (Hardness = R_c 28)

Figure 32. Structure of Nickel Modified Low Carbon (0.2%) AMS 5749: Carburized 72 Hours at 1228 K (1750° F); CP = 0.8% for 6 Hours, 0.5% for 66 Hours; Austenitized at 1339 K (1950° F); Still-Air Cooled; Tempered 783 K (950° F) 2+2 Hours.

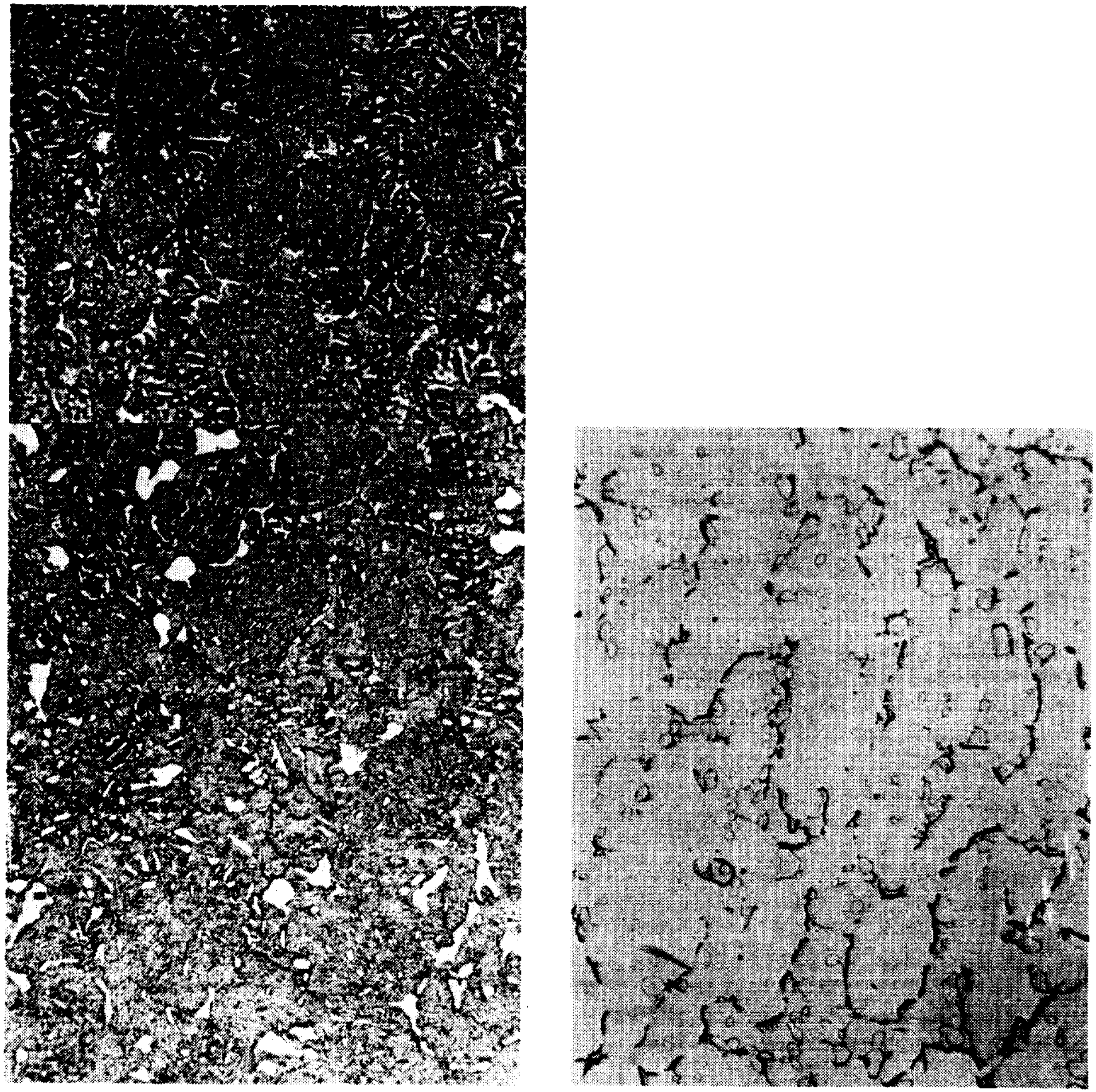

Etchant: Mod. Picral 500X

Case (Hardness = R_c 52)

Etchant: Mod. Prical 500X

Core (Hardness = R_c 32)

Figure 33. Structure of Nickel Modified Low Carbon (0.1%) AMS 5749: Carburized 72 Hours at 1228 K (1750° F); CP = 0.6% for 6 Hours, 0.5% for 66 Hours; Austenitized 1339 K (1950°F); Oil Quenched; Tempered 783 K (950° F) 2+2 Hours.

Nevertheless, due to the fact that (1) case hardnesses were still considered below desirable levels and (2) concern that the required long carburizing times would be a serious manufacturing cost and reliability problem, it was decided to halt the effort in this area. After reviewing the results with the NASA Project Manager, it was decided that one more alternate approach should be explored. This led to the evaluation of several lower chromium alloys (~14%). This effort will be discussed in the next section.

3.4 REDUCED CHROMIUM CONTENT, LOW CARBON STEELS

Since the attempts to carburize the nickel modified, low carbon AMS 5749 did not result in the desired combination of case hardness and microstructure, it was decided to explore an alternate approach. This consisted of reducing the chromium content to below 14% and adding additional molybdenum to attain chromium equivalency in corrosion. To perform this additional effort, the services of AMAX Metals Group Research Laboratory (formerly Climax Molybdenum Co. of Michigan) were enlisted. The AMAX Research Laboratory (ARL) has complete facilities to VIM-VAR melt small heats of material, as well as convert these from ingot to small diameter bar. In addition, ARL has all of the requisite analytical facilities as well as a staff of highly qualified personnel.

ARL has considerable experience with the high chromium steels for elevated temperature applications. For weldability, the carbon levels are generally kept below 0.2%, thereby automatically providing the proper carbon range for carburized material. Based on ARL's experience, it appeared that a steel with a nominal 12% chromium plus nickel and molybdenum (to provide additional corrosion protection) would provide the highest level of corrosion resistance available in an alloy that could be carburized.

ARL conducted a preliminary carburizing study on two 12% chromium steels being evaluated in separate investigations. Compositions and surface hardness data following a 7-hour carburizing cycle are shown in Table 8. Also shown are the hardness values following a subsequent 1-hour hardening treatment at 839 K (1922° F). Metallographic evaluation of the case microstructures indicated that a large volume fraction of carbide was formed during carburizing and that case depths were on the order of 0.5 mm (0.020 inch).

Table 8. Preliminary Carburizing Results of 12% Chromium Steels.

Steel	Element, Weight Percent								Carburized Hardness, HRC	Heat Treated Hardness, HRC
	C	Mn	Si	Cr	Mo	Ni	V	W		
6455	0.070	0.56	0.22	11.87	1.50	1.46	0.18	1.04	56.8	59.7
2808	0.076	0.61	0.26	12.02	1.98	5.89	0.25	---	39.5	41.0

Concerning the corrosion resistance of these materials, ARL's experience indicated that corrosion characteristics are more sensitive to the final case microstructure than to the original chromium level of the steel. Because the chromium level in solution will govern the corrosion resistance, the final heat treatment may therefore play a major role in determining how much chromium is available to prevent corrosion. For this reason, it was decided to use a maximum of 12% chromium for the current study. Higher chromium levels tend to produce a ferrite/austenite structure at the carburized surface; this could lead to chromium segregation to the ferrite phase and subsequent deterioration of corrosion properties. Corrosion test results suggested that a drop from the 14% chromium level of AMS 5749 steel to a 12% level would not drastically decrease corrosion characteristics. Consequently, both ARL and GE embarked on a survey of commercial 12% chromium steels as well as steels containing an intermediate level of 8% to 12% chromium, which might be considered as potential candidates for the intended purpose. The matrix shown in Figure 34 was constructed to provide guidance in the selection of alloys to be melted and investigated. Based on this analysis, the compositions shown in Table 9 were selected for melting.

Four 762 mm (30 inch) long [29.5 kg (65 lb)] three-way split heats were prepared as VIM-VAR material. The actual compositions of the melts are shown in Table 10.

The ingots were forged at 1473 K (2200° F) into 32 mm (1.25 inch) round bars and 13 mm (0.5 inch) round bars from which specimen blanks were cut. These blanks were processed as follows:

1. Preoxidized for 2 hours at 1253 K (1800° F)

2. Carburized in two groups as follows:

   - 7 hours at 0.5% carbon
   - 2 hours at 0.8%, 5 hours at 0.5% carbon

   The blanks were then warm oil quenched.

3. Stress relief for 2 hours at 753 K (900° F)

4. Austenitize at 1378 K (2021° F) in hydrogen for 10 minutes (warm oil quench)

5. Deep freeze and temper:

   - Two hours deep freeze (dry ice)
   - Two hours 783 K (950° F)
   - Two hours deep freeze
   - Two hours 783 K (950° F)

Surface hardness values (HRC) were obtained following Steps 2, 4, and 5 for both carburizing conditions; the results are summarized in Figure 35. Microhardness profiles obtained following Step 5 are shown in Figures 36 and 37.

	% Chromium							
		1.0	2.0	4.0	8.0	12.0	14.0	17.0
% Molybdenum	1.0			X-2(M) H-11, H-22, H-13		410, 420 SS D2, D3		
	2.0			M-50		422M SS	EX7 440C(M)	440C
	4.0	X53 CBS-100	Bower				BG42	
	6.0		H-12	M2, M3, M4 M-1, M-20				
	9.0			M-42				

Figure 34. Matrix of Chromium Steels Evaluated for Potential Corrosion Resistance.

Table 9. Compositions Selected for Melting.

Steel	Split	Mo	Ni	Cr	W
1	A	1.0	1.0	12.0	---
	B	2.0	2.0	12.0	---
	C	3.0	3.0	12.0	---
2	A	1.0	2.0	12.0	---
	B	2.0	3.0	12.0	---
	C	3.0	5.0	12.0	---
3	A	2.0	2.0	10.0	---
	B	2.0	2.0	12.0	1.0
	C	2.5	3.0	12.0	1.0
4	A	3.0	3.0	8.0	---
	B	4.0	3.0	8.0	---
	C	4.0	3.0	9.0	---
All steels to contain 0.2% C, 0.3% Si, 0.5% Mn, 0.001% S, 0.01% N, and 0.05% Al.					

Table 10. Actual Compositions of Melts.

Steel	C	Mn	Si	Mo	Ni	Cr	W
1A	0.19	0.50	0.32	1.00	1.00	12.22	NA
1B	0.19	0.50	0.32	1.94	1.98	12.22	NA
1C	0.19	0.50	0.32	2.81	2.86	12.22	NA
2A	0.19	0.50	0.33	1.02	2.05	12.09	NA
2B	0.19	0.50	0.33	1.96	3.02	12.09	NA
2C	0.19	0.50	0.33	2.71	4.54	12.09	NA
3A	0.20	0.51	0.32	2.03	2.04	10.22	NA
3B	0.20	0.51	0.32	2.03	2.04	11.84	1.03
3C	0.20	0.51	0.32	2.34	2.90	11.84	1.03
4A	0.19	0.48	0.31	3.02	3.04	8.17	NA
4B	0.19	0.48	0.31	3.92	3.04	8.17	NA
4C	0.19	0.48	0.31	3.92	3.04	8.96	NA

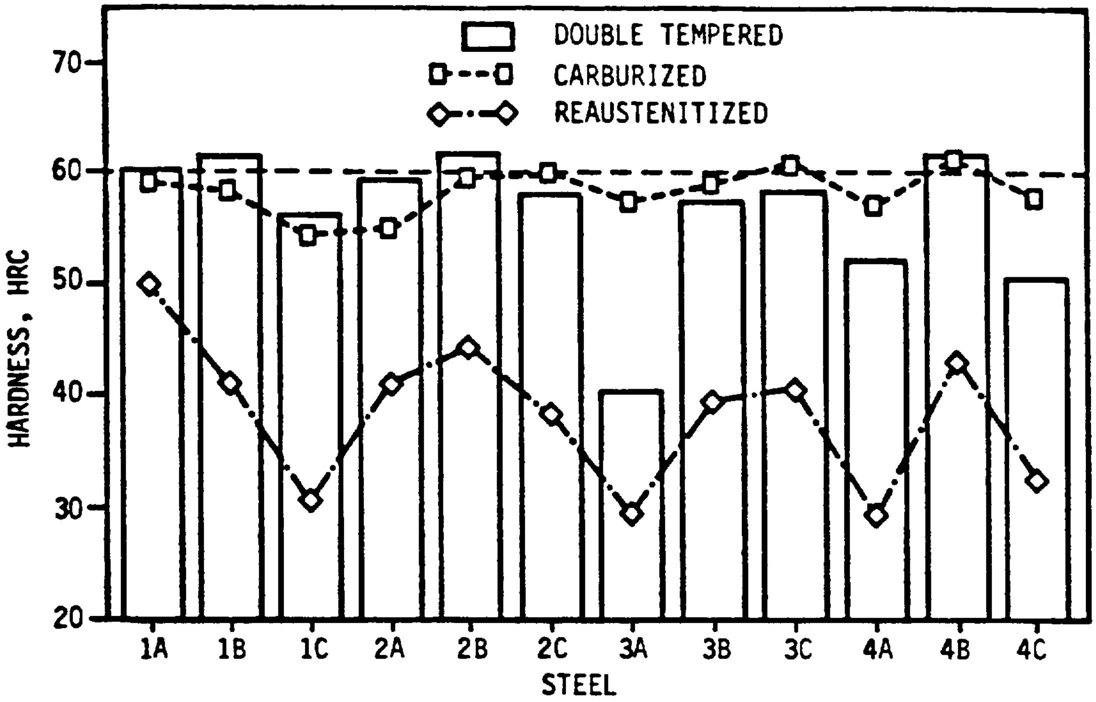

(a) Carbon Potential 0.5% for 7 hours

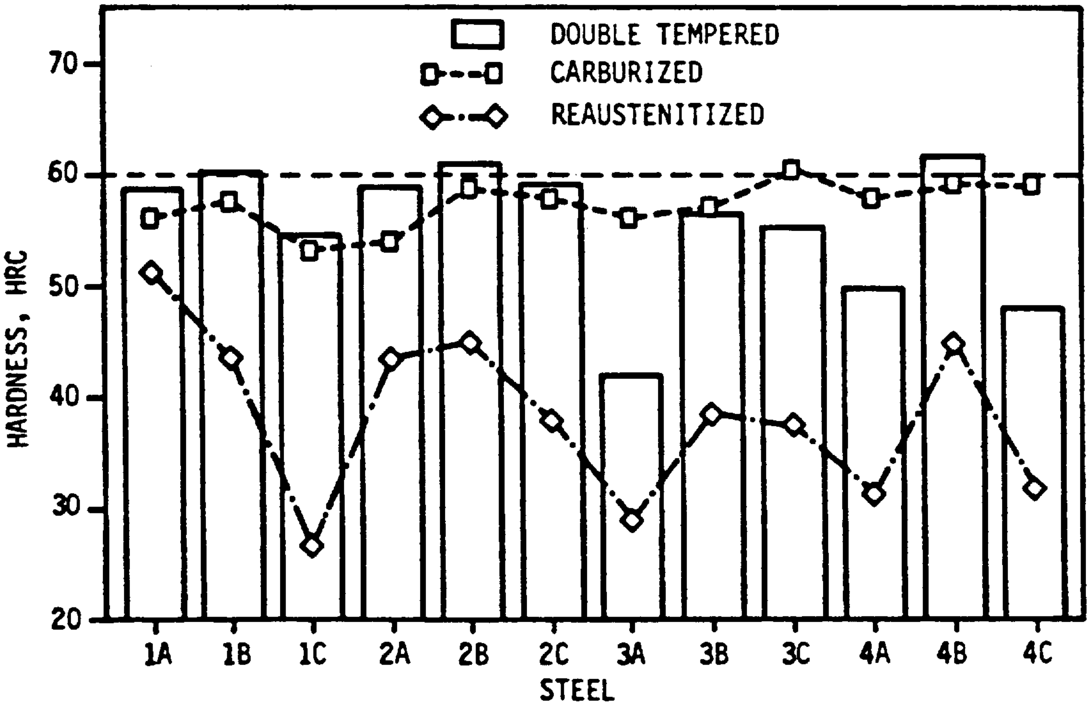

(b) Carbon Potential 0.8% for 2 hours, then 0.5% for 5 hours

Figure 35. Surface Hardness Following Various Heat Treating Stages.

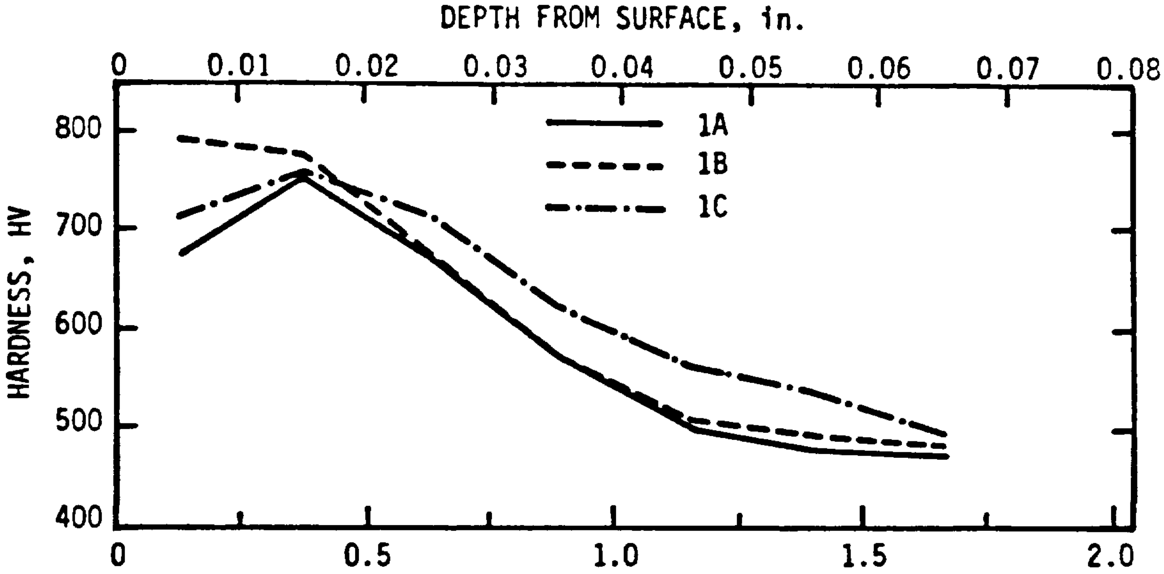

(a) Steels 1A, 1B, 1C

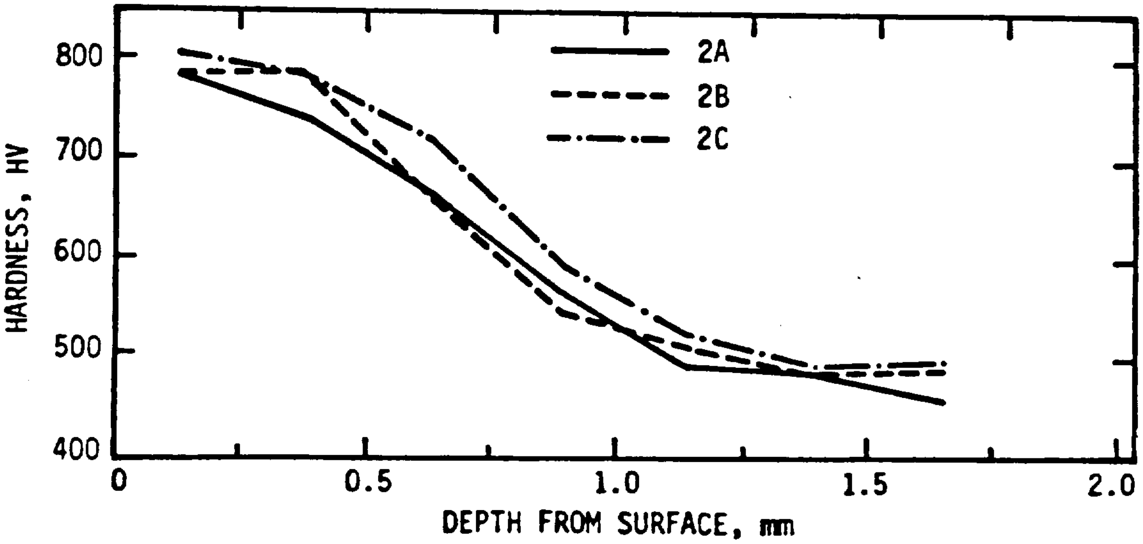

(b) Steels 2A, 2B, 2C

Figure 36. Microhardness Profiles of Steels Carburized at 0.5% Carbon for 7 Hours.

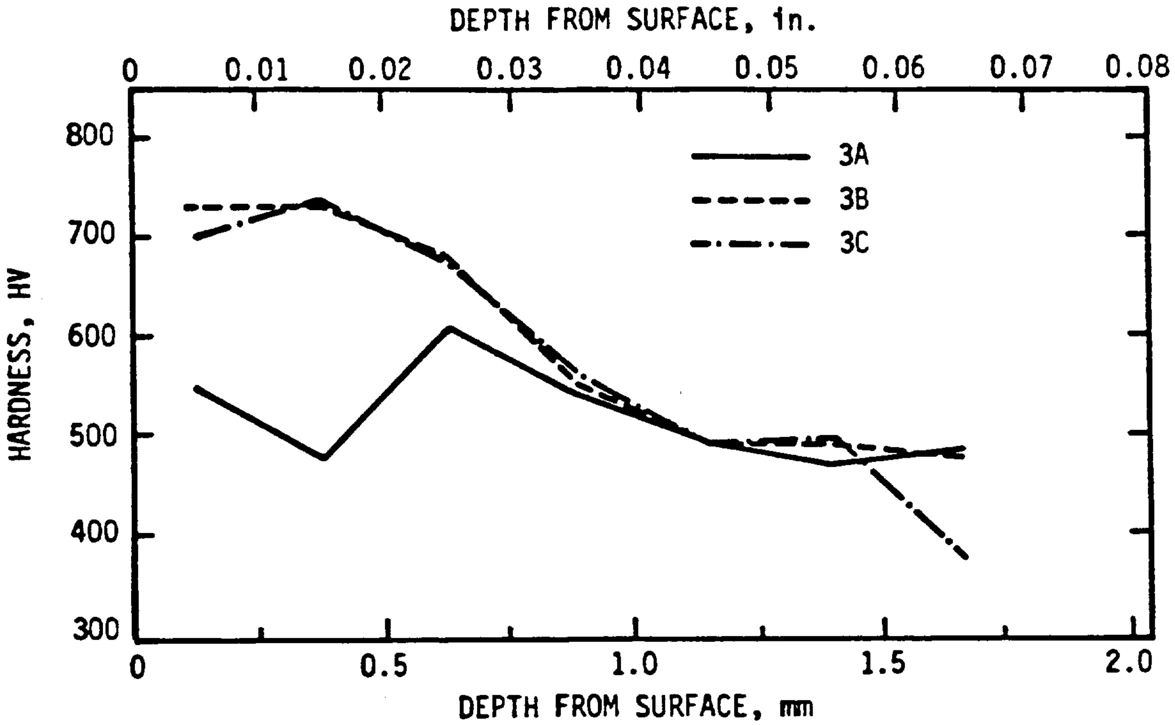

(c) Steels 3A, 3B, 3C

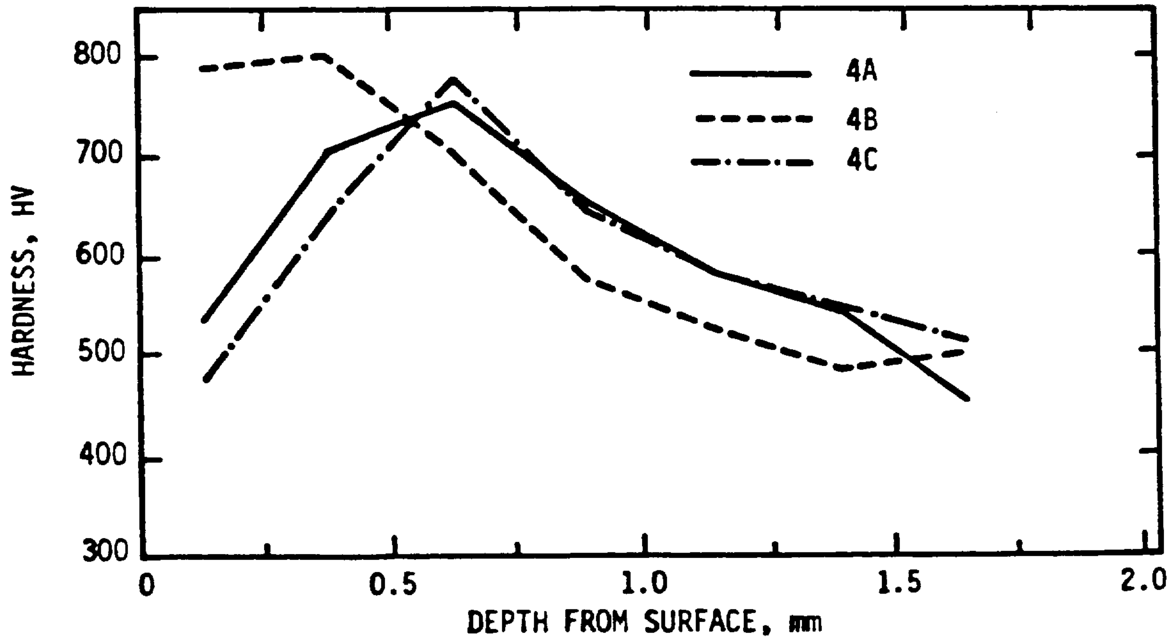

(d) Steels 4A, 4B, 4C

Figure 36. Microhardness Profiles of Steels Carburized at 0.5% Carbon for 7 Hours (Concluded).

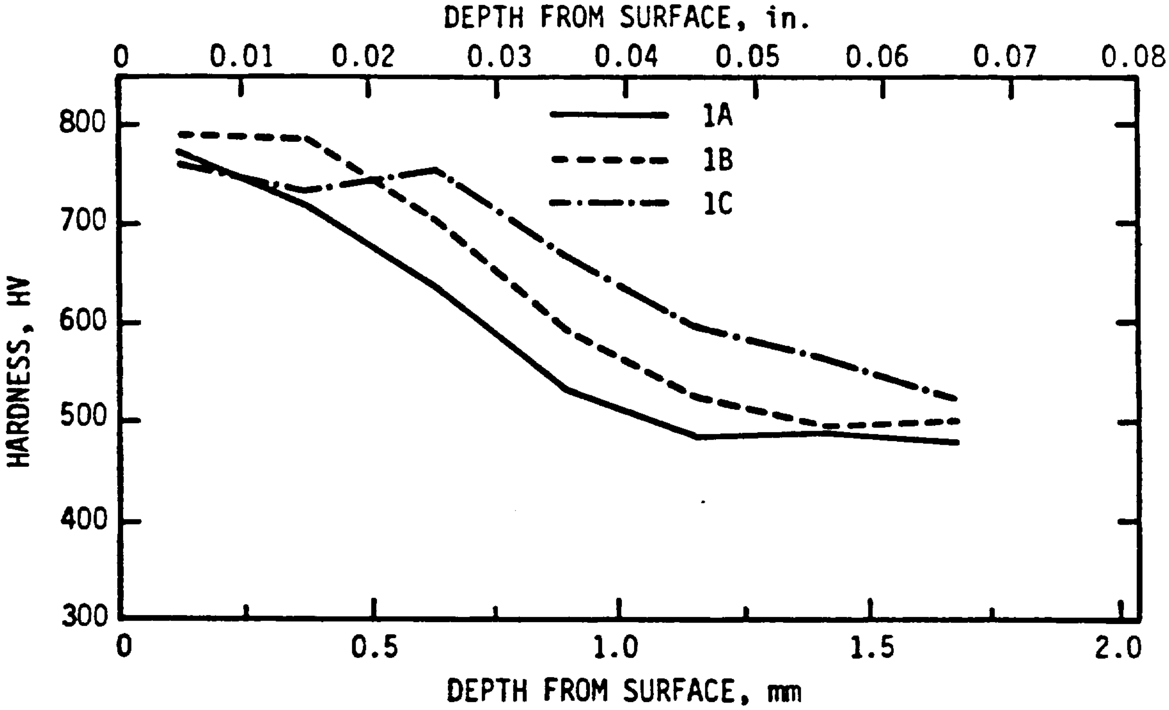

(a) Steels 1A, 1B, 1C

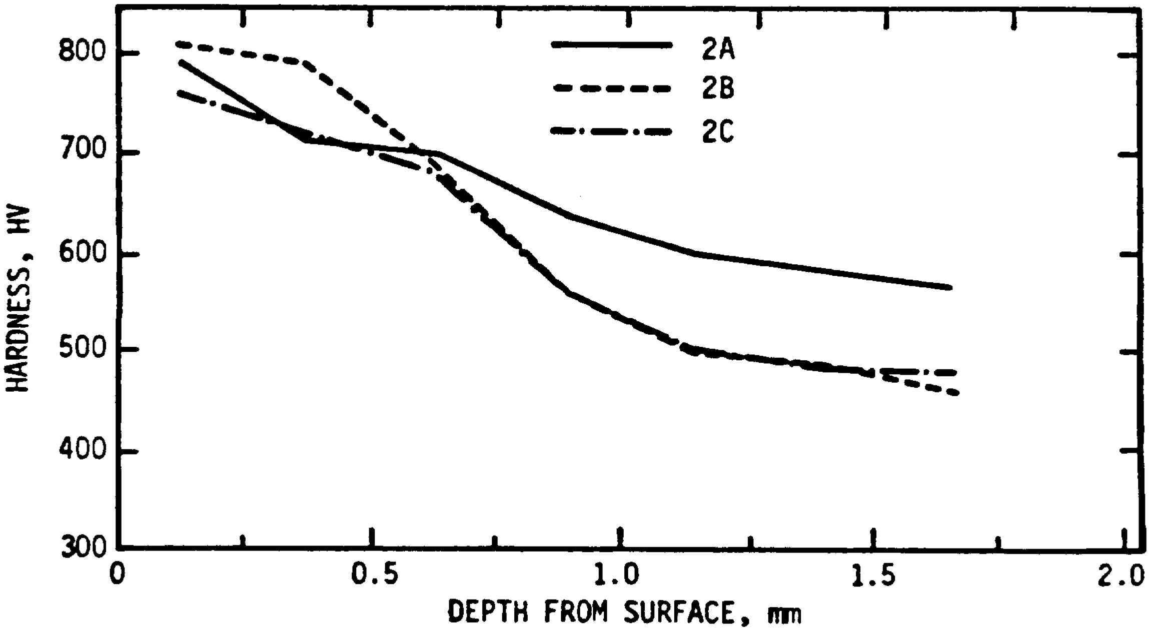

(b) Steels 2A, 2B, 2C

Figure 37. Microhardness Profiles of Steels Carburized at 0.8% Carbon for 2 Hours, 0.5% Carbon for 5 Hours.

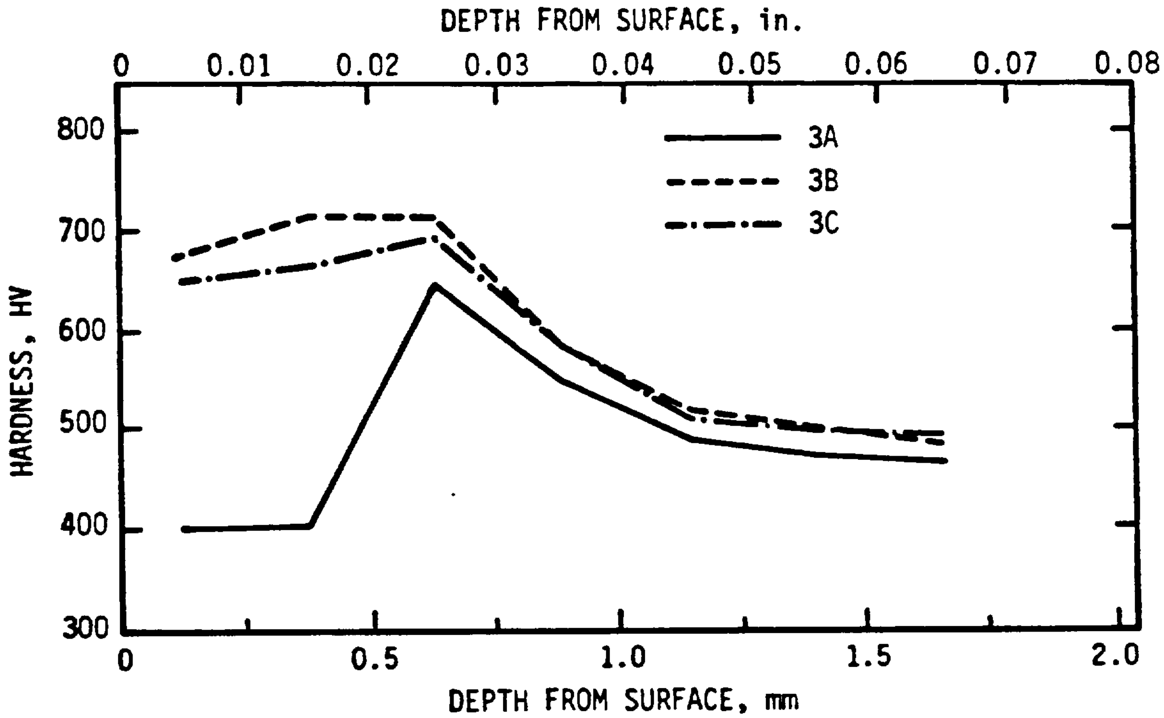

(c) Steels 3A, 3B, 3C

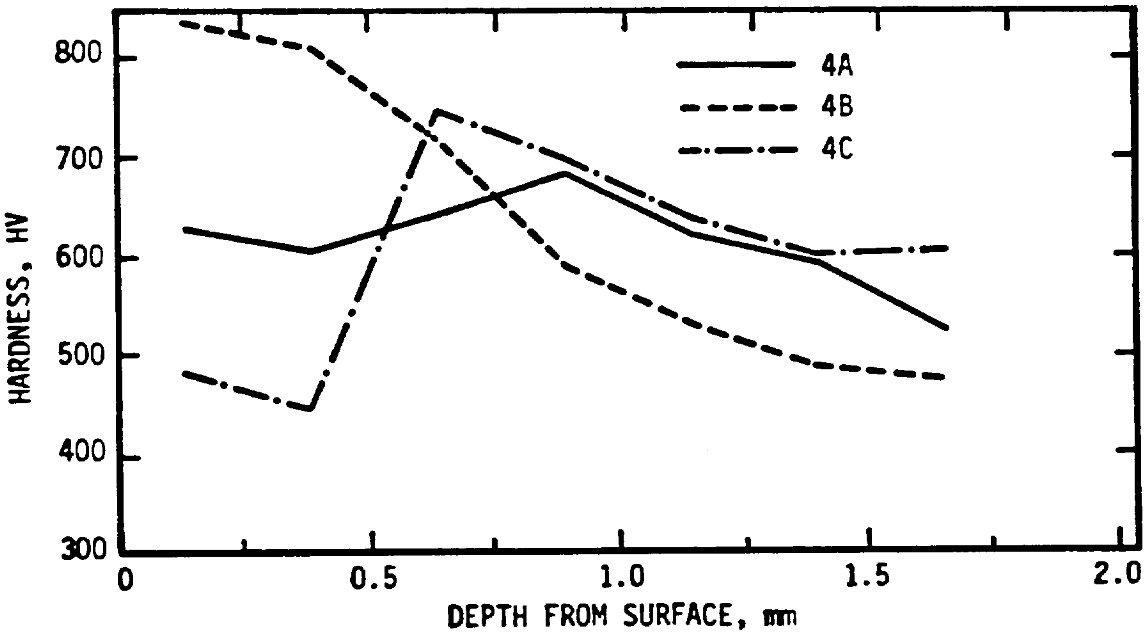

(d) Steels 4A, 4B, 4C

Figure 37. Microhardness Profiles of Steels Carburized at 0.8% Carbon for 2 Hours, 0.5% Carbon for 5 Hours (Concluded).

Based on the results shown in Figures 36 and 37 and on examination of the microstructures following Step 5, Steels 1A, 1B, 2A, 2B, 3B, 3C, and 4B were selected for further processing.

From each of these steels, rolling contact fatigue (RCF) specimens and carbon gradient bars were machined. Half of the RCF specimens had saddles machined in the surface to a depth of approximately 3.3 mm (0.13 inch). All R_c specimens and carbon gradient bars were processed (along with additional specimens for metallography purposes) according to the schedule shown above, but with the following exceptions:

Step	Revised Procedure
2	Carburized for 14 hours at 0.5% carbon
4	Reaustenitized for 12 minutes at 1375 K (2015° F) in salt

Surface hardness values following processing are shown in Figure 38 in comparison with the results obtained previously (7 hour carburization cycle). Microhardness profiles with the revised procedure are shown in Figure 39. Microstructures at a depth of approximately 0.4 mm (0.015 inch) below the carburized surface are shown in Figure 40. These specimens were heavily etched to illustrate the distribution and size of the carbide particles present.

The hardness results shown in Figure 35 following various heat treating stages indicate that, in general, the carburized and tempered hardness values were closely related, and that in most cases the "B" composition in each steel group had the highest tempered hardness value. The low hardness values of the austenitized steels are assumed to be a result of the formation of retained austenite, most of which is subsequently transformed during the tempering operation. An example of the effect of alloying is found by comparing the tempered hardness values of Steels 1B and 3A in Figure 36. The low tempered hardness values of the 3A composition are a result of higher retained austenite related to its lower chromium content. The effect of W and Mo on tempered hardness is illustrated in the comparison of hardness values between the A and B steels in groups 3(W) and 4(Mo). When chromium is lowered, the addition (or increase) of W or Mo will act to substantially increase tempered hardness values.

The hardness profiles of the 7- and 14-hour carburizing cycle samples are shown in Figures 35, 36, and 39. The differences between the two carburizing processes did not seem to produce major differences in the hardness profiles.

The comparison of surface hardness values in Figure 38 also indicated that the longer carburizing cycle did not have a consistent or major effect on the surface hardness values of the steels used in this evaluation. The values below 60 HRC are a result of the retained austenite present after tempering. An examination of the microstructures indicated that the carburized zones

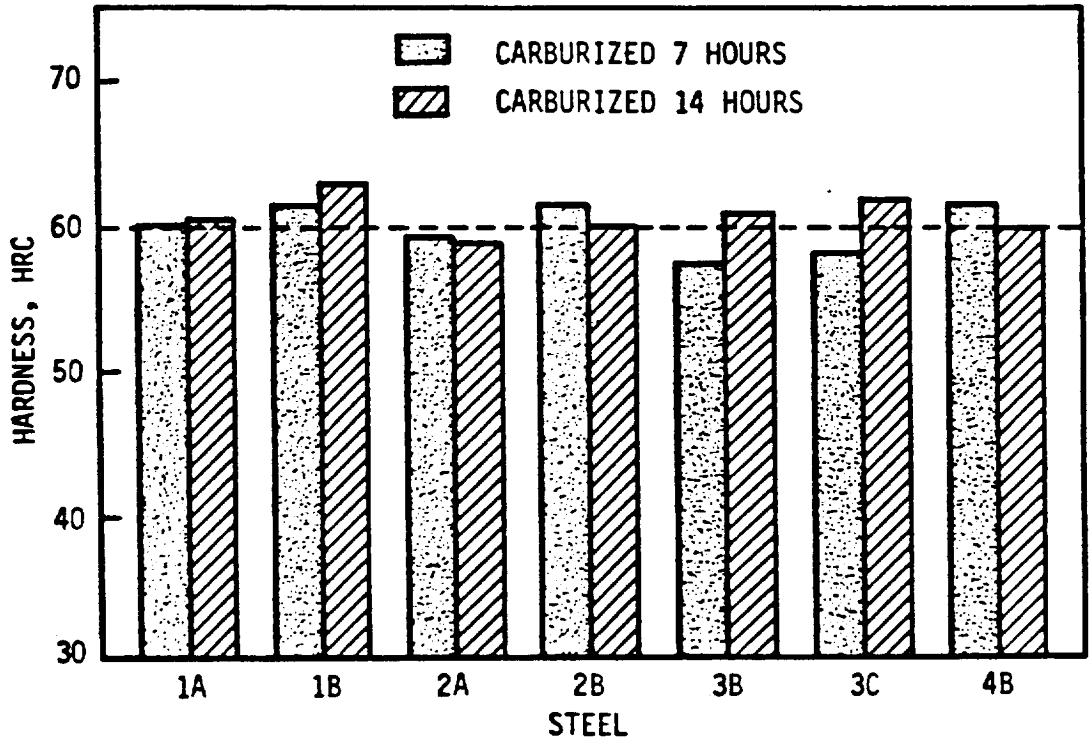

Figure 38. Comparison Between Surface Hardness Values Obtained in 7 and 14 Hour Cycles: Carburizing Potential = 0.5%; Values Were Obtained After Double Temper.

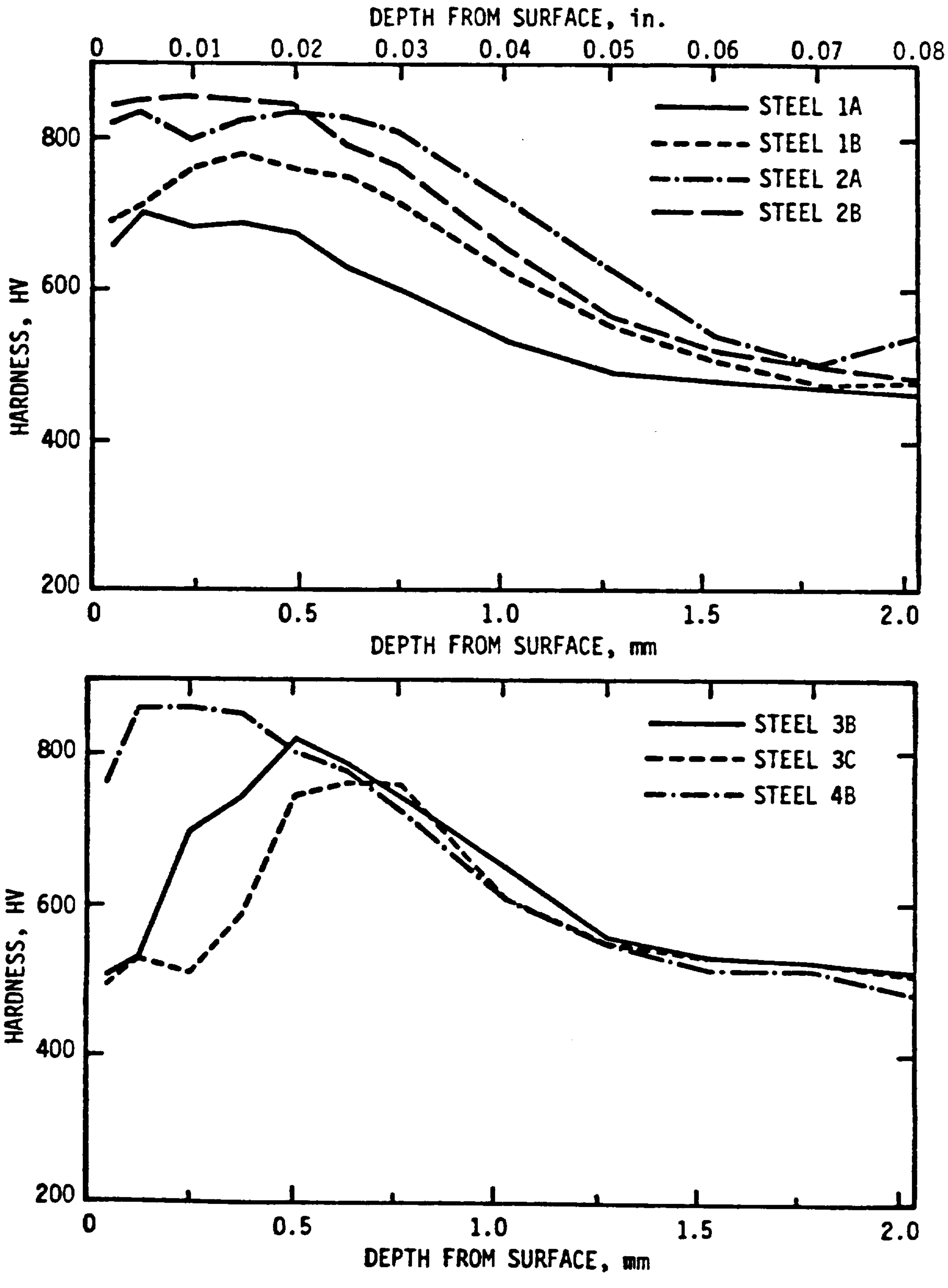

Figure 39. Hardness Profiles on Steels Carburized 14 Hours at 0.5% Carbon.

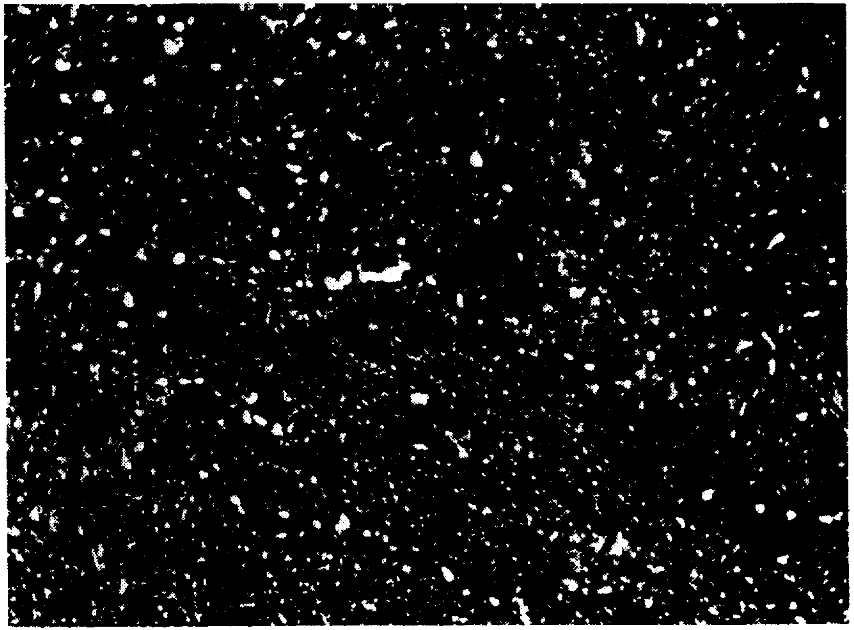

1000X

(a) Steel 1-A

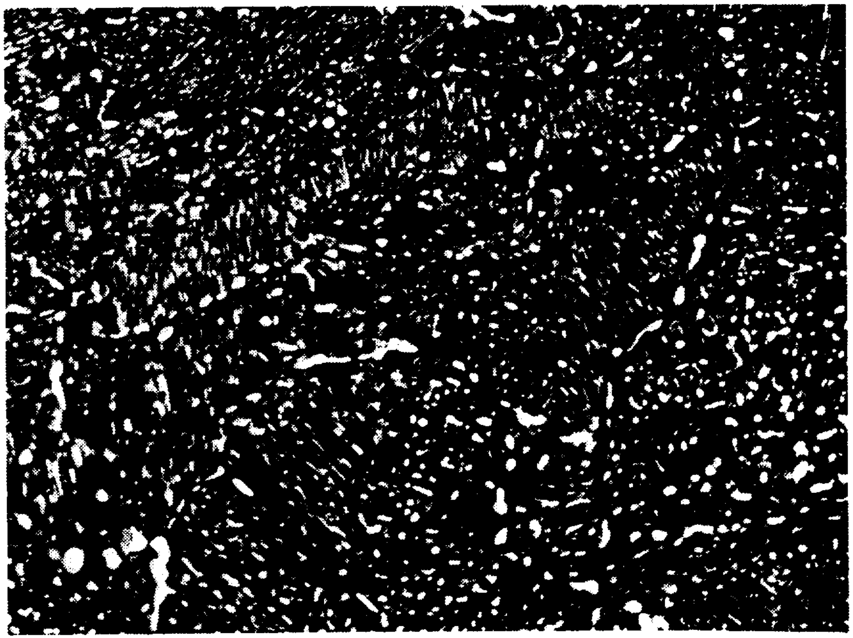

1000X

(b) Steel 1-B

Figure 40. Microstructures of Steels 1-A and 1-B Illustrating Carbide Distribution at an Approximate 0.4 mm (0.015 in.) Depth From Surface (Etchant: Vilella's Reagent).

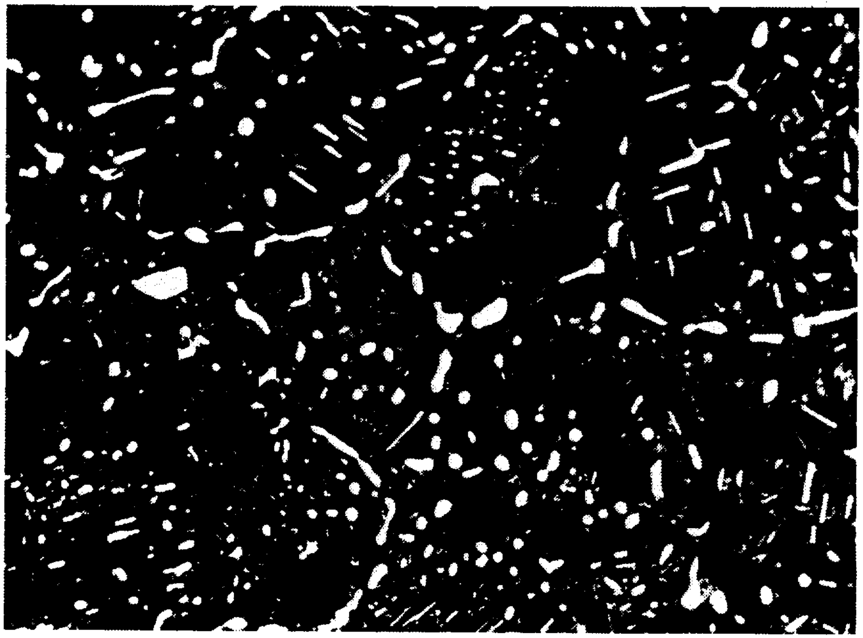

(c) Steel 2-A 1000X

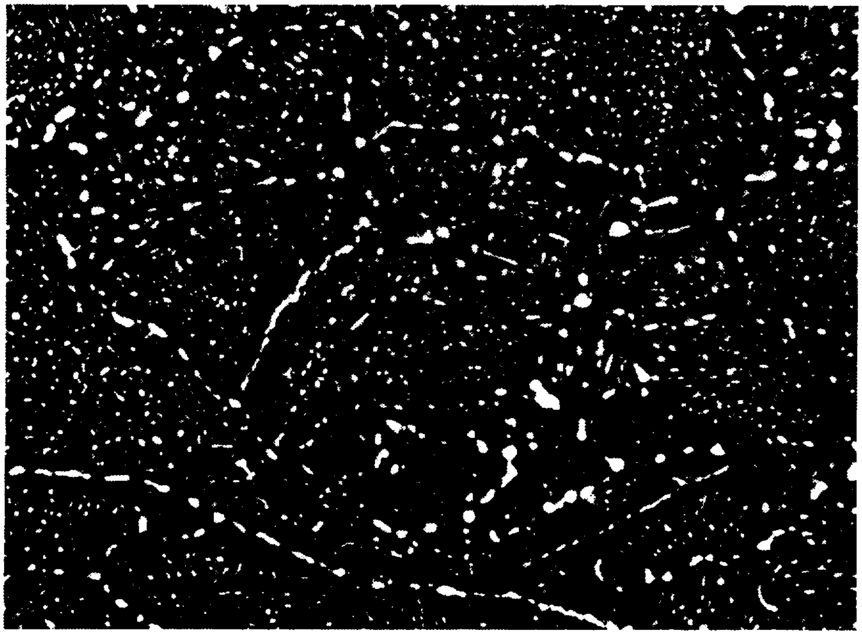

1000X

(d) Steel 2-B

Figure 40. Microstructures of Steels 2-A and 2-B Illustrating Carbide Distribution at an Approximate 0.4 mm (0.015 in.) Depth From Surface (Etchant: Villella's Reagent)(Continued).

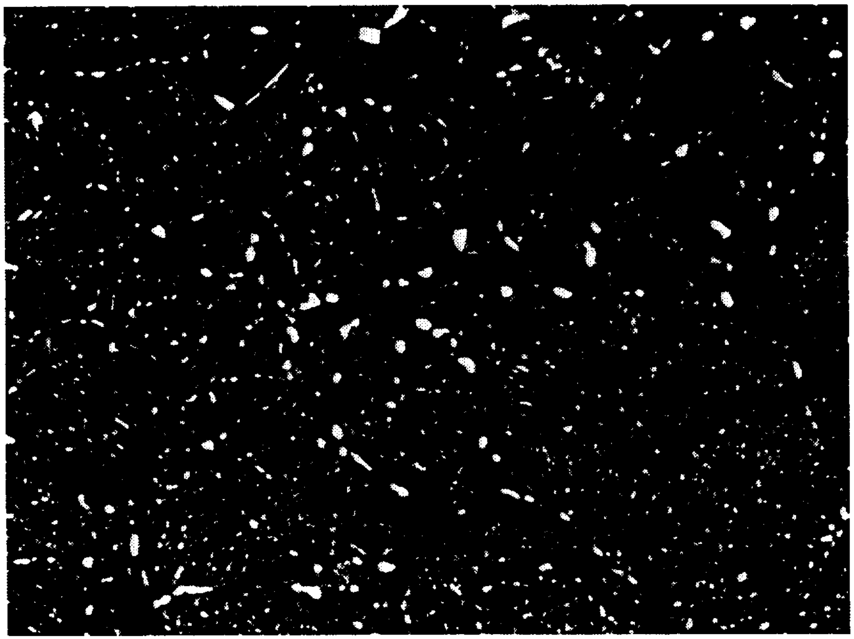

(e) Steel 3-B

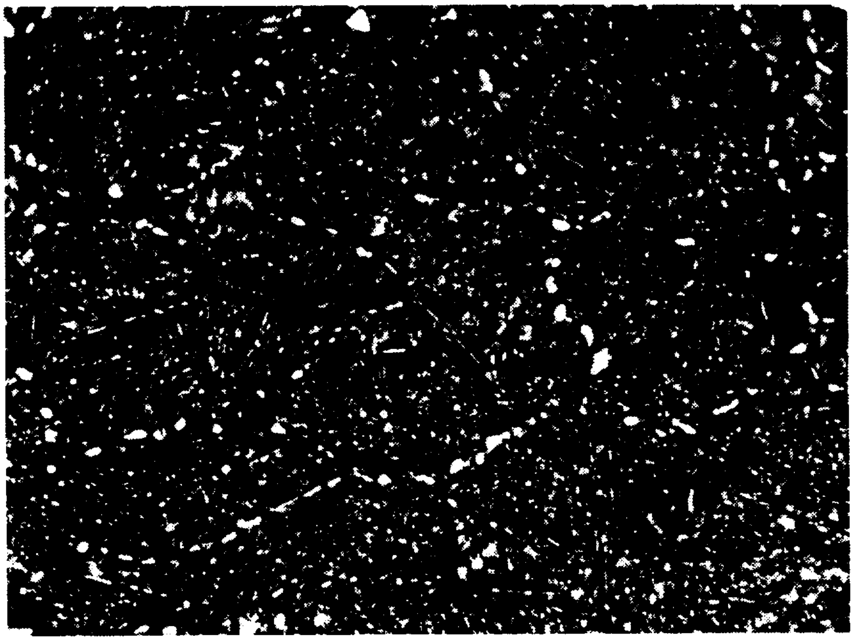

(f) Steel 3-C

Figure 40. Microstructures of Steels 3-B and 3-C Illustrating Carbide Distribution at an Approximate 0.4 mm (0.015 in.) Depth From Surface (Etchant: Vilella's Reagent) (Continued).

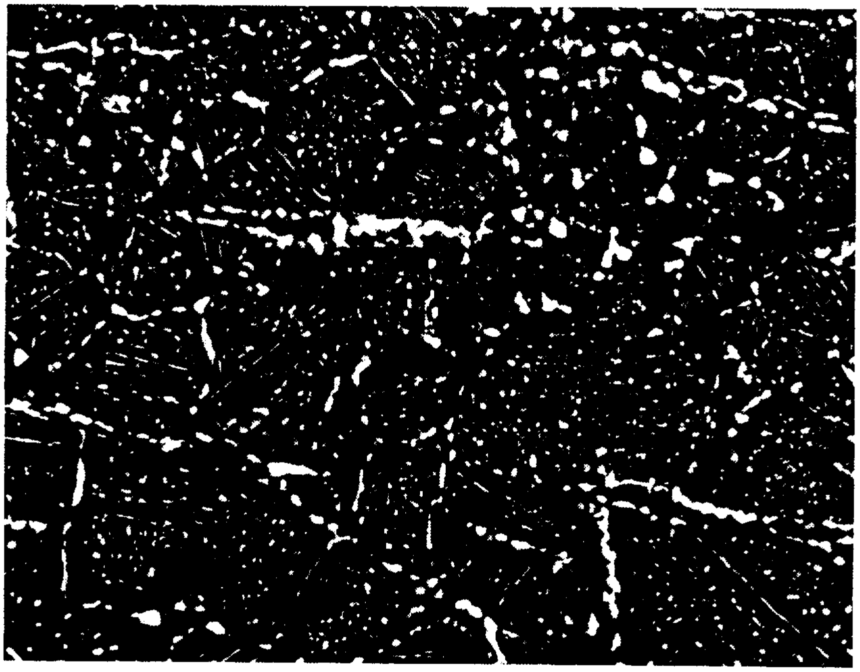

(g) Steel 4-B

Figure 40. Microstructures of Steel 4-B Illustrating Carbide Distribution at an Approximate 0.4 mm (0.015 in.) Depth From Surface (Etchant: Vilella's Reagent) (Concluded).

consisted of martensite, carbide, and retained austenite, confirming that case portions were either austenitic or austenite plus carbide at the reaustenitizing temperature.

The microhardness profiles of the 14-hour carburized samples shown in Figure 39 are generally deeper than those obtained after 7 hours of carburizing, and they suggest greater variety in hardening response than indicated in Figure 38. Figure 39 indicates that Steels 1A and 2A have the shallowest and deepest hardness profiles, respectively. In contrast, Steels 3 and 4 have similar case depths but substantially different near-surface hardness values related to the differences in retained austenite levels. The excess retained austenite at the surface may be an indication that the carbon potential was higher than it needed to be.

Grain boundary carbide networks are evident to some extent; however, the carbide morphologies observed in these steels generally appear to be not unlike those obtained in through-hardened AMS 5749 steels.

Although there was no ferrite present in the case regions of any of the steels, the core of Steel 4B indicated a dual phase (martensite plus ferrite) structure following heat treating, as shown in Figure 41. The ferrite phase was found to form in a direction parallel to the rolling direction of the bar.

In those cases where a good case structure was achieved, (that is, a structure without excessive carbide agglomeration or grain-boundary decoration), the hardness failed to meet the R_c 60 minimum. This was the case for Alloys 1A and 2B. When the desired surface hardness was attained, as in Alloy 1B, excessive case carbides were present. In the case of Alloy 3C, the low surface hardness is apparently due to excessive amounts of retained austenite.

While the hardness levels were considered marginal, the improvement in the overall microstructure (over that attainable with the modified AMS 5749) was considered sufficiently promising to conduct corrosion and RCF testing.

3.4.1 Corrosion Tests

Corrosion tests were performed on Steels 1A, 2A, 1B, 2B, 3B, 3C, and 4B using the procedure previously described. Each corrosion test fixture consisted of four bars. These bars were:

- One M50 bar - control specimen
- One AMS 5749 bar - control specimen
- Two development alloy bars

Figure 42 shows a typical corrosion test fixture configuration. In this case, the combinations were as follows:

- M50 versus AMS 5749
- M50 versus development alloy (1A)

ORIGINAL PAGE IS
OF POOR QUALITY

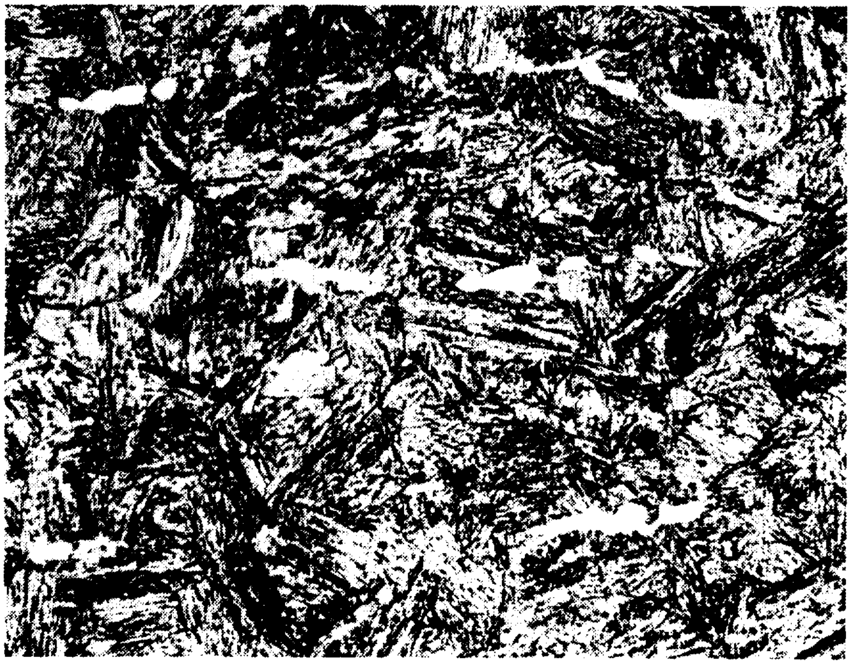

Figure 41. Core Microstructure of Steel 4-B Etchant = Vilella's Reagent.

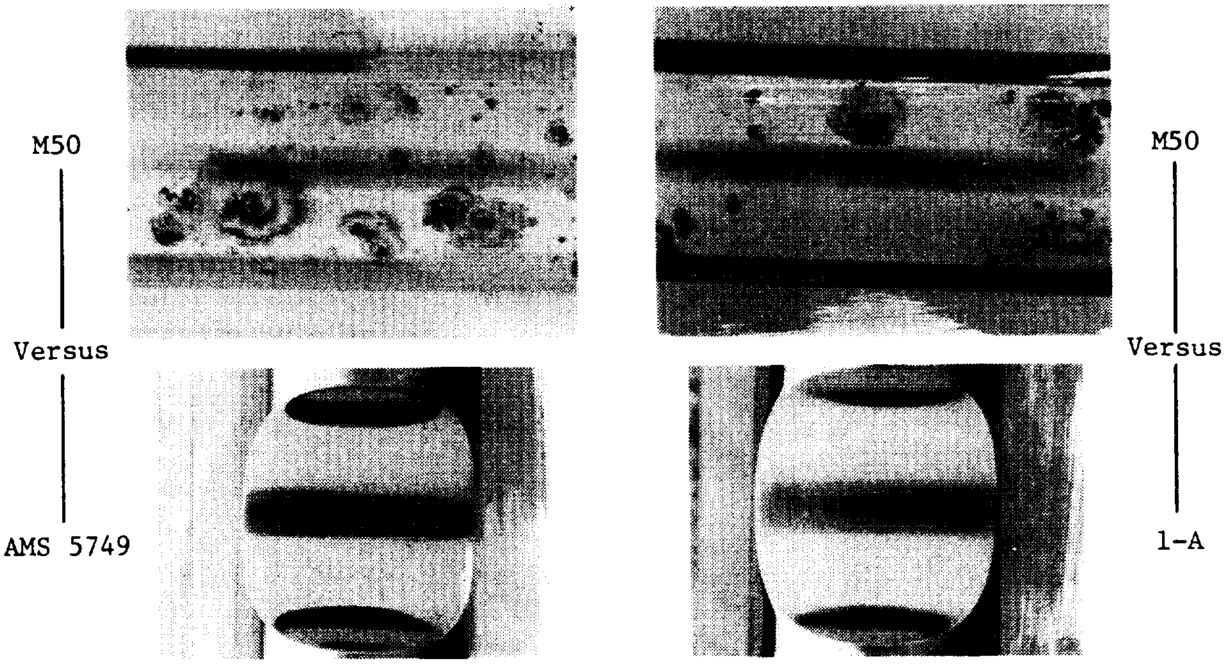

After 14 Corrosion Cycles (5X Mag)

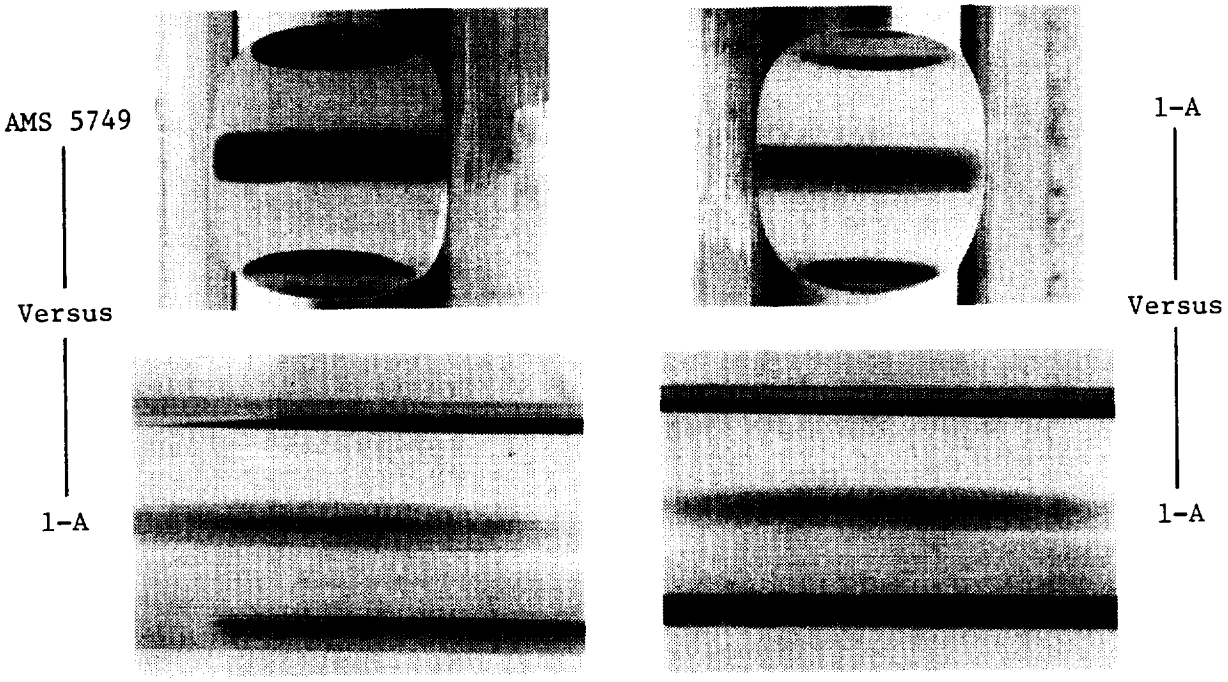

Figure 42. Typical Corrosion Test Fixture Configuration.

- AMS 5749 versus development alloy (1A)
- Development alloy versus itself (1A)

Following the corrosion tests, the bars were examined and evaluated. This consisted of a 10X examination of the bar surfaces and a documentation of the number of corrosion pits [felt with a 0.7 mm (0.03 inch) scribe] in the cylindrical areas as well as in the saddles. A summary ranking of the corrosion observations is given in Table 11. It should be emphasized again that this ranking is based on pits which can be felt with a 0.7 mm (0.03 inch) scribe, not on what is considered "cosmetic" corrosion. These observations indicated that most of the 12 chromium alloys had reasonably good corrosion resistance, except for Alloy 2B which showed a relatively large number of pits. No specific reason for this behavior has been established. Not unexpectedly, the lowest chromium content alloy (4B) had a greater number of corrosion pits.

Table 11. Corrosion Evaluation by Pit Counts.

Material	Saddle		Cylindrical Section	
	Versus Itself	Versus M50	Versus AMS 5749	No Contact
1A	0	1	0	0
2A	0	0	0	1
1B	0	0	0	1
2B	2	1	0	2
3B	1	0	0	1
3C	0	0	0	1
4B	1	2	1	2

Ranking: 0 = No Corrosion
1 = Mild, 5 pits
2 = Medium, 5 to 10 pits

3.4.2 Rolling Contact Fatigue Testing

Despite the marginal hardness levels of the 8% to 12% chromium steels, it was decided to perform some rolling contact fatigue tests using General Electric's RC Rig (Reference 16). Test conditions were as follows:

Load: 296 kg (652 lb)
Stress: 2068 MPa (700 ksi) S_{max}

Temperature: Room Temperature Ambient
Speed: 25,000 rpm (50K Stress Cycles/Minute)
Lubricant: MIL-L-23699

The RC rig test series was short-lived. Seven tests were performed on Alloys 3C, 3B, and 2B. The results were as follows:

Alloy	Cycles	Results
2B	105×10^6	Spalling
3C	144×10^6	Suspension
3C	144×10^6	Suspension
3C	144×10^6	Suspension
3B	144×10^6	Suspension
3B	144×10^6	Suspension
3B	144×10^6	Suspension

Visual examination of the running track showed significant plastic deformation on all bars, thereby indicating that the hardness of these specimens was insufficient to carry the applied load. Surface profile measurement confirmed this observation, as shown in Figure 43. For comparison, Figure 44 shows surface traces made on through-hardened VIM-VAR M50 and case carburized M50NiL. While the running track can also be seen on the latter, the amount of deformation is very small (~50 µm). Thus, while the bars from Alloys 3B and 3C reached the suspension point of 144×10^6 cycles, the results are not considered reliable. The reason is that because of plastic deformation, the conformity between the RC roller and the test bar continually increases. This increases the contact area and decreases the Hertzian stress, thus making the test invalid.

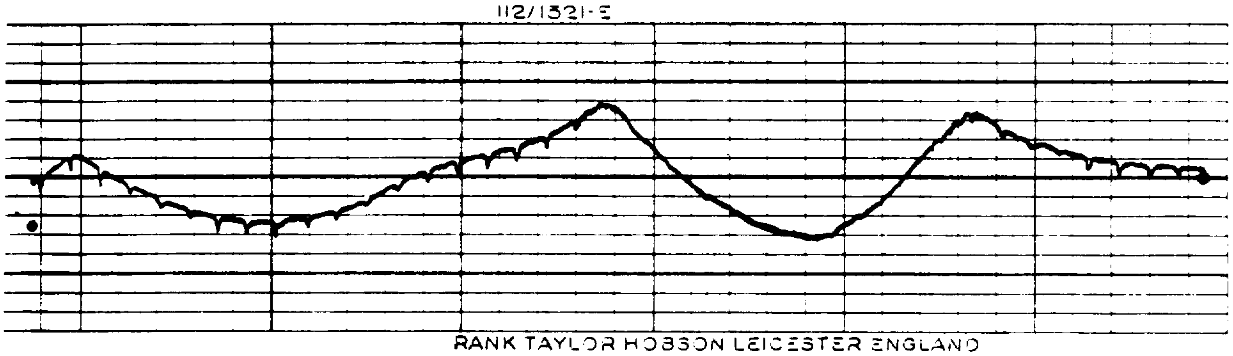

3C Track 1, 84 x 10^6 Cycles

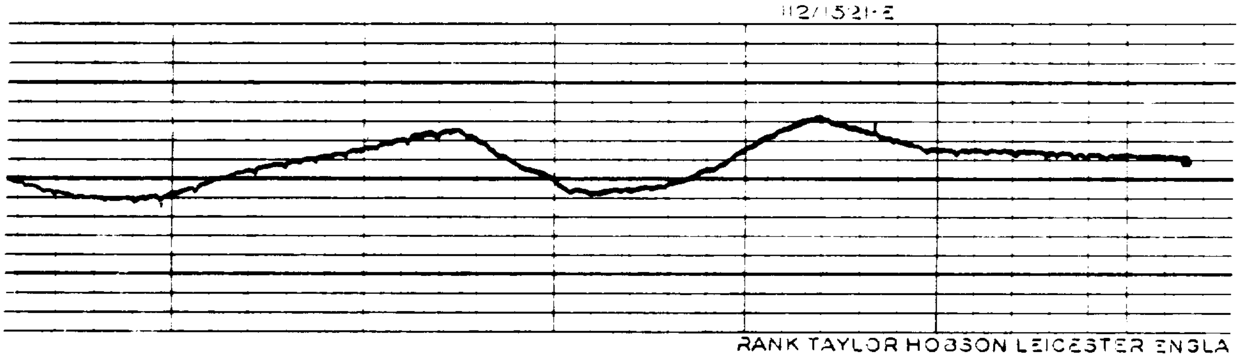

3B Track 1, 144 x 10^6 Cycles

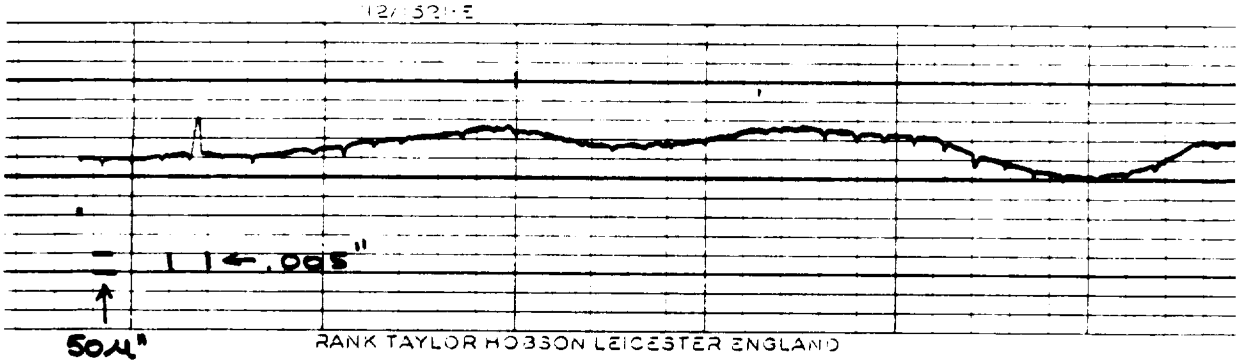

2B Track 3, 144 x 10^6 Cycles

Figure 43. Deformation in AMAX Bars.

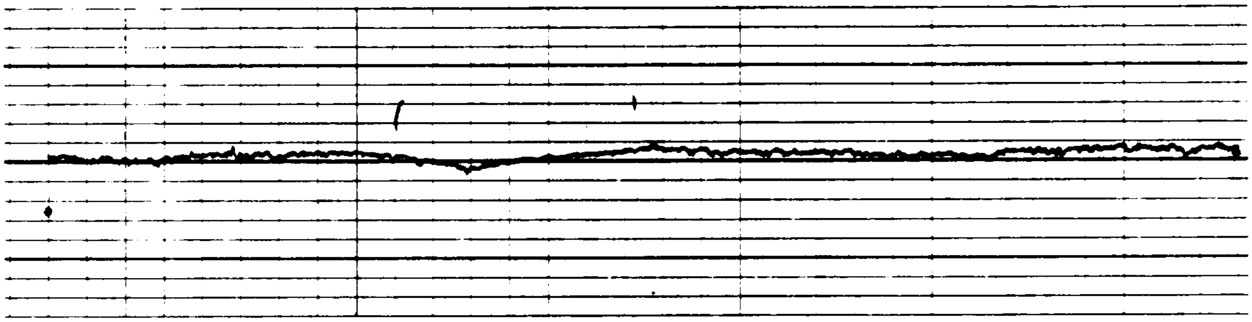

M50 Standard Bar 144 x 10^6 Cycles

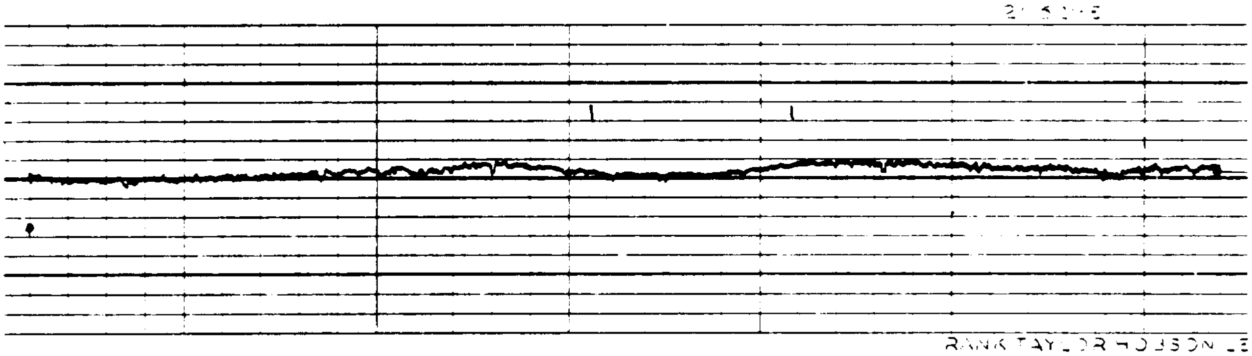

M50NiL 144 x 10^6 Cycles

Figure 44. Surface Profile of M50 Standard and M50NiL R_c Bars.

4.0 CONCLUDING REMARKS AND SUMMARY OF RESULTS

The primary objective of this program was to link the corrosion resistance of a high chromium steel with the excellent fracture resistance possible with a case-carburized material. It was recognized at the outset that this was a difficult technical problem due mainly to the difficulty of properly carburizing a relatively highly alloyed material. The primary objective was not achieved despite several alloy modifications beyond those originally envisioned for this effort. As pointed out in the body of the report, the major obstacle was achieving an acceptable combination of case hardness and microstructure and, to a lesser degree, a good core structure. An acceptable minimum case hardness was defined as HRC 58 to HRC 60. An acceptable case microstructure for rolling element bearing application is a structure free of massive carbide agglomerations or carbide networks and having relatively small, well-dispersed carbides in a fully martensitic matrix.

The initial effort which consisted of reducing the AMS 5749 carbon content from about 1.1% to 0.1% did not approach the overall objective because of the presence of excessive retained austenite in the carburized and hardened samples. This precluded reaching even the minimum case hardness requirement.

The second iteration, consisting of adding 3% nickel, produced some results which were quite close to the desired combination of case hardness and structure. Nearly 200 carburizing and heat treat cycles were performed in this phase with the best results obtained with a boost-diffuse cycle, a relatively low carbon potential (ranging from 0.5% to 0.8%), and employing a fairly rapid quench after the austenitization cycle. In this report, only typical examples of the results achieved are shown since it would be rather redundant, if not numbing, to present all of the results in this study. Perhaps the closest to achieving the desired objective were the results shown in Figure 26. The carbides are relatively small and dispersed, and the hardness is just HRC 58. However, the core structure is an approximate 50/50 mix of low carbon martensite and ferrite - a structure which would not be expected to provide outstanding fracture toughness.

In the final modification, which consisted of reducing the chromium level, the results again were promising but not to the point of fully meeting the program objective or warranting the commitment of resources to evaluate the materials in full-scale bearing tests.

It could be argued that the original requirements were unduly restrictive or that some of the test conditions were too severe. Certainly, the high Hertzian stresses imposed by the RC rig, which in turn demand a relatively high hardness to sustain these stresses, is a severe test and in actual bearing operation, where stresses are considerably lower, an R_c 58 hardness might be adequate. However, it must be recognized that a comparison needed to be made with existing bearing materials which have demonstrated millions of successful flight hours at hardness levels in the range of HRC 60-64. Any reduction in these hardness levels would make this comparison less meaningful.

Despite the fact that the primary goals were not achieved, much useful data have been generated regarding the feasibility of carburizing high chromium steels. Additionally, the corrosion evaluation of the AMS 5749, AISI M50, and AISI 52100 has provided the first such direct comparison of these materials.

5.0 REFERENCES

1. Cunningham, J.S., Jr., and Morgan, M.A., "Review of Aircraft Bearing Rejection Criteria and Causes," Lubrication Engineering, Vol. 35, No. 8, 1979, pp. 435-440.

2. Jones, H.F., "Discussion of Review of Aircraft Bearing Rejection Criteria and Causes," Lubrication Engineering, Vol. 35, No. 8, 1979, pp. 441.

3. Brown, C., and Feinberg, F., "Development of Corrosion-Inhibited Lubricants for Gas Turbine Engines and Helicopter Transmissions," Lubrication Engineering, Vol. 37, No. 3, 1981, pp. 138-144.

4. Bieberich, M.J., Brown, C.L., and Limpert, J.C., "Development of Corrosion Inhibited MIL-L-23699 Oils for Naval Aircraft and Transmissions," D.W. Taylor Ship Research and Development Center, DTNSRDC/SME 80/36, 1980.

5. Fontana, M.G., and Greene, N.D., Corrosion Engineering, McGraw-Hill, New York, N.Y., 1978.

6. Hubler, G.K., Hirvonen, J.K., Singer, I., Gossett, C.R., Clayton, C.R., Wang, Y.F., Munson, H.G., and Kulhman, G., "Application of Ion Implantation for the Improvement of Localized Corrosion Resistance of M50 Steel Bearings," Naval Research Laboratory, NRL-MR-4481, AD-A097230, 1981.

7. Parker, R.J., and Hodder, R.S., "Rolling-Element Fatigue Life of AMS 5749 Corrosion Resistant, High Temperature Bearing Steel," J. of Lubr. Tech., Vol. 100, No. 2, 1978, p. 233.

8. Valori, R., "Discussion of Rolling-Element Fatigue Life of AMS 5749 Corrosion Resistant, High Temperature Bearing Steel," J. of Lubr. Tech., Vol. 100, No. 2, 1978, p. 233.

9. Brown, P.F., and Potts, J.R., "Evaluation of Powder Processed Turbine Engine Ball Bearings," AFAPL-TR-77-26, 1977.

10. Parker, R.J., "Rolling-Element Fatigue Life of AMS 5900 Balls," NASA TP-2080, 1983.

11. Bamberger, E.N., "Materials for Rolling Element Bearings," Bearing Design - Historical Aspects, Present Technology and Future Problems, Edited by W.J. Anderson, ASME H00160, 1980.

12. Bamberger, E.N., Averbach, B.L., and Pearson, P.K., "Improved Fracture Toughness Bearings," AFWAL-TR-84-2103, January 1985.

13. Parker, R.J., Bamberger, E.N., and Nahm, A.H., "Corrosion of Simulated Bearing Components of Three Bearing Steels in the Presence of Chloride-Contaminated Lubricant," Lubrication Engineering, Vol. 40, No. 5, May 1984.

14. Kulman, G.R., "Discussion to Development of Corrosion Inhibited Lubricants for Gas Turbine Engines and Helicopter Transmissions," Lubrication Engineering, Vol. 37, No. 3, 1981, p. 143.

15. Briggs, J.Z. and Parker, T.D., "The Super 12% Cr Steels," Climax Molybdenum Co. of Michigan, 1965.

16. Bamberger, E.N., and Clark, J.C., "Development and Application of the Rolling Contact Fatigue Test Rig," From Rolling Contact Fatigue Testing of Bearing Steels, ASTM STP 771, 1982.

1. Report No.
NASA CR-174990

2. Government Accession No.

3. Recipient's Catalog No.

4. Title and Subtitle
Improved Fracture Toughness Corrosion
Resistant Bearing Material

5. Report Date
August 1985

6. Performing Organization Code
R86AEB104

7. Author(s)
E.N. Bamberger and A.H. Nahm

8. Performing Organization Report No.

10. Work Unit No.

9. Performing Organization Name and Address
General Electric Co., Aircraft Engine Business Group
1 Neumann Way
Cincinnati, Oh 45215

11. Contract or Grant No.
NAS3-22508

13. Type of Report and Period Covered
Final Report
1981 - 1984

12. Sponsoring Agency Name and Address
National Aeronautics and Space Administration
Washington, DC 20546

14. Sponsoring Agency Code

15. Supplementary Notes

Project Manager: Mr. Harold H. Coe, Rotorcraft Section, Propulsion Systems Division,
NASA-Lewis Research Center, Cleveland, Ohio 44135

16. Abstract

A development program was performed to establish whether a corrosion-resistant bearing material, such as a 14Cr steel, could be modified to allow carburization, thereby providing the excellent fracture toughness characteristics feasible with this process.

The alloy selected for investigation was AMS 5749. Several modifications were made including the addition of a small amount of nickel for austenite stabilization. While some promising results were achieved, the primary objective of an acceptable combination of case hardness and microstructure was not attained.

Because the high chromium content presents a serious problem in achieving a viable carburizing cycle, a number of experimental steels having lower chromium contents (8%-12%) were produced in laboratory quantities and evaluated. The results were basically the same as those initially obtained with the modified AMS 5749.

Corrosion tests were performed on AMS 5749, AISI M50, and 52100 bearing steels as well as some of the lower chromium steels. These tests showed that a reduced chromium level (10%-12%) provided essentially the same corrosion protection as the 14Cr steels.

17. Key Words (Suggested by Author(s))
Bearing, Corrosion, Fatigue,
Fracture Toughness

18. Distribution Statement
General Release
Star Category: 37

19. Security Classif. (of this report)	20. Security Classif. (of this page)	21. No. of Pages	22. Price*
Unclassified	Unclassified	81	$3850

* For sale by the National Technical Information Service, Springfield, Virginia 22161